Dear Editor, dear Reviewers,
the authors wish to thank both reviewers for careful reading of the manuscript, helpful remarks and constructive criticism. We want to precede this response by a somewhat general explanation of our modeling concept that appears to have caused a great deal of misunderstanding -- likely due to somewhat unspecific model motivation in our paper: Our goal is not to fit an aquifer model to the really existing subglacial aquifers by finding correct geometrical and physical parameters. This approach would likely work for flows through till or similar types of drainage but just as likely fail for channel networks. Instead we chose Darcy model as an 'idealized' representation of all drainage processes (including channels) and tuned it to give the best fit to the available data. This, in particular, means that channels are not being explicitly modeled (and hence no channel equations are being used) but, instead, the effect of channel drainage is represented by appropriately chosen hydraulic conductivity coefficients in the framework of the Darcy equation. To better explain this point, we added a corresponding sentence to the introduction.

We also want to clarify that not representing cavities in our model does not mean that we not aware of numerous sophisticated studies on cavity formation that appeared in the past decades, but rather state that our focus is the channels that clearly top our priority list -- partly due to our studies of 79NG in which we have been looking for a long time for locations where field studies could potentially survey subglacial channels.

In general, many points raised in the reviews, are highlighting that (more) observations of subglacial hydrology underneath ice sheets are urgently required.

Technicalities: below we answer each point raised by the reviewers and mark our answer in blue color, whereas the original comment of the reviewer is shown in black. Point raised by both reviewers are answered at one location and referenced at the second one.

We have performed the following major changes - that are all also documented below in detail:

- **Appendix A - presents the derivation of the channel opening and closure terms**
- **We improved the discretisation of v_melt term to prevent occurrence of checkerboard patterns and rerun all simulation**
- **In Eq 10, we changed b to min(b,h-z_b) as suggested by the reviewer**
- **We moved the numerical discretisation description into the Appendix B**

First review

D. Brinkerhoff

Specific Comments

Model formulation

I appreciate the novel thinking showcased in this paper; it's always useful to approach an old problem in a new way, and by switching from the classical model formulation used in most contemporary ice sheet models to this new viewpoint, the authors certainly introduce a new way of thinking.

1) Unfortunately, I think that this viewpoint lacks physical justification. The primary way in which this paper departs from previous subglacial hydrology modelling efforts is that differences in flux are accounted for by changes in the conductivity, rather than a change in the average cavity size. However, the equations for evolving cavity size (which are well understood from a theoretical perspective) are used to model the change in conductivity, with units made to match by simply multiplying by the conductivity. How is this justified? Without any theoretical justification, the model becomes strictly heuristic, and if this is the case, why is this model formulation any better than any other random model formulation that happens to achieve results that compare favorably to SHMIP? If the authors can provide such physical justification, I will happily withdraw this criticism. If not, then I want to see this point stated prominently in the paper.

In order to address the concerns about a our model being heuristic, we provide the derivation of Eq. 9: The key parameter describing the efficiency of drainage is the transmissivity that is computed as the product of the conductivity with the effective layer thickness (Eq. 4). Thus, mathematically speaking, it is fully equivalent whether we model the conductivity with fixed thickness (as in our study) or other way around (as was done in de Fleurian et al. 2016). To supplement this, we added Appendix A to the revised manuscript describing the derivation of the melt and creep terms.

To sum it up, in terms of physical foundation, we generally stay very close to modeling approaches used in de Fleurian et al. 2016 with the main difference being not the representation of cavity size /effective conductivity relationship, but the use of a single Darcy layer capturing both drainage systems instead of relying on two distinct layers with rather complex coupling conditions between them.

2) There is a sign error in Equation 9: the creep term should be negative.

Thank you for pointing it out. This was just a typo in the manuscript, the code is using the correct sign. We have changed it accordingly in Eq. 9.

3) Also, v_{melt} as written implies that melt is always based on a fully saturated aquifer. The b in that term should be replaced with $min(b, h)$.

This is correct, we did not account for that until now. We have updated this in our model and re-run the experiments. However, the impact of this change in our setups was negligible.

4) Coupling to basal sliding

The chosen formulation neglects the coupling between sliding and hydrology. Most models of subglacial hydrology allow for the opening of cavities (and hence an increase in the effective transmissivity) by accounting for ice cavitation over sub-grid scale bedrock asperities. In contrast, this paper assumes that transmissivity (what I can only view as a proxy for the opening of cavities or channels) opens only by dissipative melting. This is problematic for several reasons. First, if the authors don't think that this is an important mechanism in making space for water to move around in below a glacier, then they need to say so. Essentially all work on this subject recognizes this as a major process, particularly in cases with significant sliding. Second, it is fairly well understood that in the continuum approximation, when this term is dominant, the problem always leads to runaway channelization, precluding the presence of linked cavities (hence the use of edge-based formulations for modelling channels in e.g. Werder (2013)). Why is this not a problem here, in both a numerical and a physical sense? Finally, the paper includes an extra parameters K min, which makes it so that there is always transport capacity, and this is identified as a sensitive parameter. This parameter strikes me as a hack to solve a problem that would be solved in a more principled way by including a term that increases conductivity proportionally to sliding Speed.

Indeed, our model does so far not include any opening of cavities, which we plan as one of the next extensions of the model. If we incorporate cavity opening, we will, however, face the challenge that the size of undulations is not known from observations at the resolution that is required. The basal roughness is typically measured with radio echo sounding and hence, depending on the instrument, one may end up with vertical resolution between 5m and 50m for airborne applications. So, once we incorporate this for artificial geometries into our model, we will lack the observations of basal undulations for real world applications. Here we would need to come with some assumptions on roughness again, which then not too much different from using a K_min that only mimics a transmission through cavities. So in some way, we account for this by having a K_min, which does allow a minimum transmission of water.

Fowler (1987) discussed the potential for cavitation in ice sheets and glaciers and found that cavitation is ruled out for large ice sheets, due to the slope of ice sheets and the length scale of bed undulations. This is likely to be valid for the major part of the ice sheets, while at the margins situation might become closer to valley glaciers in terms of surface slope. The NEGIS itself exhibits, however, also quite some surface undulations, so a cavity model would be definitely interesting to apply to this area.

One could, on the other hand, also argue that there are no direct observations of subglacial channels in Greenland and question, based on that, their role as a key component of the hydrological system. Indeed, the only observation we are aware for the surface representation of a subglacial channel drainage might be p. 13 of http://old.esaconferencebureau.com/Custom/14C19/Presentations/02%20day%202%20(Wednesday,%2017%20September)/Session%207/1440_Nagler.pdf giving an indication of width and size of subglacial channels without being a real in-situ observation of a subglacial channel. Existence of subglacial channels is on the other hand also consistent with the observation of plumes in fjords at tidewater glaciers and would also be consistent with findings of melt channels underneath the floating tongue glaciers, e.g. Petermann and 79NG. Thus we were targeting channels rather than cavities in our model first.

We discuss the issue of runaway instability further below (see 4) in the second review).

Bindschadler 1983, ''The Importance of Pressurized Subglacial Water in Separation and Sliding at the Glacier Bed, Journal of Glaciology, Vol 29, No 191, p. 3-19
Fowler 1987, "Sliding with cavity formation" Journal of Glaciology, Vol 33, No 115, p. 255-267

5)Transmissivity formulation
The principle variable entering the mass conservation formulation is h, defined as the piezometric head, or the potential relative to some fixed datum. This is fine, so long as the appropriate modifications are made when the head drops below the bedrock elevation (this does not seem to be handled at all in this model).
We do handle this problem via the unconfined aquifer formulation and illustrate this in Section 3.2: without the unconfined formulation, the head drops below the bedrock, which leads to negative water pressure. When considering the transition to unconfined aquifer, as soon as the head drops below the top of the aquifer, the transmissivity is reduced, reaching zero when the head reaches the bedrock. This prevents it from dropping below the bedrock. This may have been unclear because of our erroneous formulation of transmissivity (see next comment), and we added a note to make this clearer:
"This also prevents the head from falling below the bedrock, as we detail in Section 3.2."

6) However, the transmissivity $t(h)$ is formulated as if h were the height above bedrock. Either the transmissivity should be $T(h) = \{K(b-B),\ h \geq b;\ K(h-B),\ B < h < b;\ 0,\ h < B$ and b should be redefined as the aquifer thickness plus bedrock elevation, or h should be redefined as the local height above bedrock and the mass conservation equation should be changed to $S_e h_t = \nabla \cdot T(h)\nabla(B+h) + Q$
Note that this error makes no difference when the bedrock elevation is uniformly zero

(SHMIP, for example). However, it would lead to some very questionable results when there are significant variations.

Thank you for pointing this out. We had it correctly in the code (same formula as the first suggestion) and now corrected the formulation in the paper by replacing h by $\Psi = h - z_b$ defined as the height of the head above bedrock.

7) Effective storage coefficient

Why does b appear in $S_e(h)$? If $h > b$, then the head is rising through glacier ice with permeability S_s (this is regularization to make the equation parabolic rather than elliptic, see Schoof (2012)). Why then would the head increase depend at all upon the thickness of the underlying aquifer?

S_s is not the permeability of the glacier ice in our model but rather the specific storage of the aquifer under the glacier that we use as an idealized model of the drainage system. In this idealized model, the effective behavior in the confined case is modeled according to the aquifer equations (and thus depends on b). Just as pointed out by the reviewer, it can also be considered as a small regularization parameter adding some elasticity to the model in the confined case. Also see our answer to 9) below.

8) It is also worth noting that S_s as presented has units that don't make sense ($Pa^{-1}m^{-1}$), and that the porosity ω cancels out in Eq. 2.

There was a typo in Eq. 2, missing a '+'. It should read $\rho_w \omega\, g\, (\beta_w + \frac{a}{w})$.

9) I also think that there is a misunderstanding with respect to the meaning of the effective storage coefficient. This is simply the void space in the aquifer versus in the glacier: it makes sense to say that the aquifer is more porous than the glacier (i.e. the head changes faster in a confined aquifer than an unconfined one), but not that more water is released from an unconfined aquifer than a confined one.

We agree that 'released' is not really a good term to describe this term and changed the formulations in the paper accordingly. However, the idea of glacier 'storing' water is not connected in any way with our modeling assumptions (or with our interpretation of S_s). The idealized model represents the main effective properties of the *entire* system that are then modeled using aquifer equations.

10) Discretization

Given that you're using central differences and forward Euler to discretize (not exactly revolutionary), this section could be moved to an appendix or supplement, or even omitted altogether.

We moved the section to the Appendix B.

11) What cannot be omitted is a discussion of stability under time stepping. In particular, the Courant-Friedrich-Lewy criterion imposes a time-step restriction for stability in the case of explicit time steps. For the chosen discretization, it is very small indeed. I would like to see some verification that the CFL is being respected. I suspect that it is currently not, which would provide a potential explanation for the obvious oscillations (i.e. checkerboard pattern) that appear in the results.
We do compute our time steps so that the CFL-criterion is always respected and plan to improve the model by using an implicit time-stepping method in the future.
We have now found the cause of the oscillations: The flux that governs the melt term is computed in the center of the cell, while the correct position would be at the boundary between cells; this lead to the observed instability. Once we changed the stencil for v_{melt} accordingly, the instabilities went away. The new results have slightly smoother distribution of K, but the general behaviour is the same as before.
We re-run all simulations with the new formulation and updated our paper accordingly.

12) Also, how bad is the mass conservation problem? If a considerable amount of mass is being lost or gained, then this affects the validity of the results.

The error in mass conservation is very small. Below is a figure for the evolution of water mass in the system for the SHMIP experiment (using our default parameters), where W is the water that is stored in the aquifer.

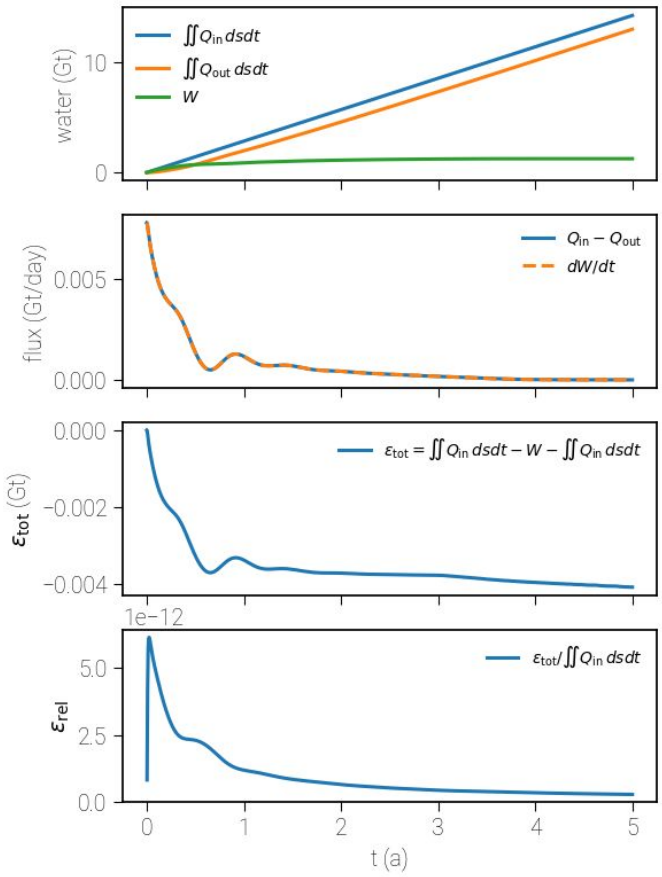

13) Parameter choices

The choices of ω and b are incompatible in most plausible scenarios for a glacier base.

In the case of a sediment aquifer, then a value of b = 10 m is reasonable, but ω = 0.4 (40% void space!) is not at all reasonable. Conversely, if the 'aquifer' is the linked cavity/conduit system, then ω = 0.4 might be reasonable but b = 10 m is too large by an order of magnitude. A much stronger effort needs to be made to state the type of physical system that the model is supposed to simulate, and parameter values with regards to this need to be better justified.

As already mentioned before, our model parameters (including aquifer geometry) are not directly related to the measurements of an actual subglacial aquifer but rather represent an 'idealized' aquifer that would display characteristics similar to the drainage system we try to simulate. Since this drainage system includes both types of transport mechanisms, the chosen parameters reflect this duality.

14) Figure 3j

Is there any transport between channels? It doesn't seem like it from this figure. Shouldn't efficient channels reduce the pressure, causing water to flow in laterally, eventually leading proximal channels to merge?

There is some transport between the areas of high conductivity seen in Fig. 3j (we do not model channels explicitly). However, these areas do not merge in this experiment probably because of the strong forcing of constant moulin supply and flat bedrock. Note that in the updated results, the areas of high drainage are more spread out.

15) N_{HUY}

The use of 'reduced ice overburden pressure' as a comparison in this case is a bit of a straw man. As it appears in Huybrechts (1990), this refers to a water pressure given by bedrock elevation below sea level, which is only reasonable when very little basal or surface melt is expected (as in the Antarctic context for which it was initially used). For NEGIS, a much more defensible comparison would be that the water pressure is bounded below by sea level height, but that otherwise it is a constant fraction of overburden.

We agree that there are other appropriate sliding parameterisations that could be used for a comparison; however, our intention was to select one of those that survived over a long time period and is still present in models participating in initMIP Greenland in order to allow the colleagues to assess how their own parameterisation is benchmarking against the application of CUAS and if using CUAS would be beneficial for their models. For this purpose, we would prefer to keep the comparison to Huybrechts approach; however, we are flexible and would remove it on advice from the editor.

16) Also, isn't $N^{-1}_{CUAS} / N^{-1}_{HUY} = N_{HUY} / N_{CUAS}$? Why the exponents?

We chose this description because sliding laws depend on 1/N, and we wanted to show where CUAS leads to more sliding, but we agree that the suggested changes make the presentation clearer.

17) On the definition of 'improvement'

What constitutes an improvement per 'we can considerably improve the velocity field in ISSM ...'? An improvement with respect to the eyeball norm? Or is it possible to be

somewhat more quantitative, e.g. computing the misfit between these results, PISM, and ISSM without the hydrological model?

Indeed the eyeball norm is not quantitative enough for this comparison. Here, we present the mean (Δ v = mean(abs(v_mod-v_obs)), the Pearson correlation coefficient, as well as the l2 norm (RMS) of the difference between simulated and observed horizontal velocities for all three cases presented in the manuscript:

Experiment	RMS (m/a)	r^2 (Pearson)	Δ v ($l1$ norm) (m/a)
ISSM Huybrechts	176.83	0.69	90.13
PISM	132.05	0.84	65.42
ISSM CUAS	126.86	0.80	53.28

We incorporated this also in the manuscript.

Technical corrections

P1L16 Citation needed

We incorporated the following references:

Lliboutry, 1968; Röthlisberger, 1972

Gimbert, F., V. C. Tsai, J. M. Amundson, T. C. Bartholomaus, and J. I. Walter (2016), Subseasonal changes observed in subglacial channel pressure, size, and sediment transport, Geophys. Res. Lett., 43, doi:10.1002/2016GL068337.

P2L1–3 Citations needed

We added the following references:

Aschwanden 2016

Van den Broeke et al. 2017

P2L24 How do you know that this strategy captures the overall behavior?

We feel that our efforts to compare our results to the available benchmarks and indirect measurements (surface velocities of ISSM) (Sections 3 and 4) do justify this claim.

P2L30 Should cite Schoof (2012) or Bueler (2015) or some other paper that discusses the implications of assuming that the system is always full

We add "This problem has been analyzed in detail by Schoof (2012), but here we study the effect in the context of equivalent aquifer models using unconfined flow as a possible solution." after the sentence.

P3L20 This statement is not true in the subglacial hydrology literature

We deleted this statement.

P16L16 Citation needed

The role of subglacial hydrology in the genesis of ice streams in general is not well understood yet.

We did not find an appropriate reference for this - papers are either proposing subglacial lakes playing a major role (e.g. Bell et al. 2007, Fricker et al., 2014), while the studies testing this hypothesis in depth are currently under review or white papers, e.g. the proposal for EGRIP, stating it as we do in this manuscript. In case the editor or the reviewers have a suggestion, we will incorporate this.

P16L32 Should be 'bed model of Morlighem (2014)' rather than 'data'. The results of a PDE-constrained optimization scheme are not data

Done.

P19L14 What does 'empirical nature' mean?

We replaced this by "its relative simplicity and representation of the main 'bulk' properties of the drainage system with a small number of tunable parameters can be an advantage.

P19L17 Not sure that 'restitution' is the right word.

Changed to 'decline'.

Second review

Efforts to parameterize the subglacial system in a simple, computationally efficient manner are important for incorporating subglacial hydrology into modelling studies covering large spatial and temporal scales. The work of the authors is novel and addresses an important area of research.
However, I have several concerns that the authors should to address.

1) Assumption of till

I think an implicit assumption in the model is a soft-bed subglacial hydrology system. This should be clarified. Since the model is applied to Greenland, I think it would be relevant to briefly cover literature discussing whether a soft-bed system exists there, since there is disagreement about the nature of the bed. This could include recent seismic studies, and touch upon the previous modelling studies making this assumption (e.g. Bougamont et al, (2014)). Further, it may also be beneficial to readers to discuss the relationship between till and sliding laws.
We do not assume any type of subglacial system in particular but aim to develop a general parametrization for different types of systems in a simplified way. For the sliding law discussion, also see 4) in the first review.

2) Model Formulation

The model description is unclear about how to conceptually understand this model. I am puzzled about the motivation and physical interpretation of scaling K with channel opening/closing while the aquifer is unconfined. This would imply that channels are forming in the porous medium? The equations for channels are not applicable there.
The interpretation of K (and its dependence on the channel opening/closure) does not differ between the confined and unconfined cases. No channels are explicitly formed, instead the conductivity is adjusted to account for the effect of both drainage systems (and, yes, we do allow the efficient drainage system to form in the unconfined case). We added some more specific conceptual explanations for our modeling approach to the introduction (also see the general comments at the beginning of this document).

3) I'm perplexed since I would expect K to be constant (or perhaps depend on other variables like strain rate, stress, sediment properties) in the unconfined case, and then force a switch to channelized behavior once the aquifer becomes confined.
K is not the intrinsic permeability but hydraulic conductivity. The former does, in fact, depend on the solid and fluid parameters. The latter is an 'effective' parameter that describes the current ability of the porous medium to conduct fluid (this includes the channels, etc.). The behavior of K that accounts for melt/creep is also assumed to be present in the unconfined case.

4) In your model formulation, you scale conductivity (Eq 9) using the equations for channel opening/closing. However, wouldn't it be more appropriate for K be scaled such

that flux through a grid cell scales to flux through an idealized channelized system? In other words, I would expect an attempt to scale ∇ ·(T(h) ∇ h) with discharge through channels (using an assumed channel spacing). Where the discharge through channels is (e.g. Equation 3 from Hewitt (2013))

$$Q = - K_c S^{(5/4)} \left| \frac{\partial \varphi}{\partial s} \right|^{(-\frac{1}{2})} \frac{\partial \varphi}{\partial s}$$

We assume a parameterization for our v_melt term following de Fleurian et al. 2016, where the discharge is given by Darcy's law as $Q = T \nabla h$ (also see our new appendix on the derivation of the parametrization). The channel equations are not applicable in our case since they would describe the effective behaviour of the drainage system in a principally different way from the Darcy law used in our model.

5) When channelization is introduced into models, they can grow unstably and dominate the system as effective pressures in channels decreases with increasing input. This doesn't appear to occur in your model. You should give a physical description of the terms (and point out the terms in your equations) preventing this.

This is an excellent point that, in fact, demonstrates one of the advantages of our modeling approach vs. explicitly resolving the channel networks. Just as pointed out in the reviewer's remark, increasing input leads to merging and thus to a lower flow resistance, this positive feedback can easily lead to instabilities. Due to combining unconfined with confined aquifers, an increase in input can be readily redistributed to available empty space in the unconfined parts (or to the outflow boundary if the aquifer is fully confined). Thus P_w rarely rises above P_i in Eq. 8, and this means that v_{creep} provides a good control on runaway hydraulic conductivity.

6) The argument that the amount of water released from an unconfined aquifer is larger than a confined aquifer is counterintuitive (P4L5). If the head drops 1m in the unconfined case, than wouldn't the water released be much greater than in the confined case, due to the volume of water in the latter being limited by the porosity?

See our answer to 9) in the first review.

7) Numerics

Your conductivity doesn't appear to show grid convergence, even at resolution of 500m. However, I would expect large scale model runs to require convergence at much coarser resolutions.

With the updated solutions (see next answer) we have much better grid convergence.

8) While you identify the conditions under which you get the checkerboard pattern, you don't really explain what is causing it to form. Is this not an artificial pattern due to the numerics? You're solving a highly non-linear equation. In a second order discretization, the dominant truncation error is odd (third order), and hence the error generally will behave in a dispersive manner. Equations 7 and 8 suggest that N ~ Pi_i – h. Since N

appears smooth in your plots, this implies h should be smooth, and then I'm uncertain why K isn't smooth as well.
We have found the cause of the oscillations: See the response to 11) in the first review. We updated our paper accordingly.

9) Application to NEGIS

Your study domain encompasses areas of both fast flow and slow flow. While the assumptions of the SSA are valid for the ice stream itself, the SSA is not the right approximation for ice flow over the majority of the domain. This is evident in Fig 10a, where we can see that your modelled ice speed is ~1 m/a over the majority of the domain. Over this part of the domain, internal deformation is the key component of ice flow. The comparison of panels A and B in Figure 10 shows not only the effect of subglacial hydrology, but also of different ice physics. Aschwanden et al. (2016) use a 'hybrid' model described in Bueler and Brown (2009), which is itself an approximation (in effect) to the Blatter-Pattyn approximation. It is worth noting that other 'hybrid' approximations exist, such as L1L2 or that of Goldberg (2011). Because of the different regimes in your domain, I think it is necessary to either use a hybrid approximation (if it's available in ISSM), or Blatter-Pattyn to test the results of your coupled model.
We fully agree with the reviewer, that SSA is not valid for the whole modeling domain. Either a so-called hybrid model (which is not available in ISSM) or a HO model would be more appropriate. However, we think just for the sake of demonstration that our simple approach is fair. In particular, we aim to show an improvement in the fast flow regions where the SSA is valid.
The PISM results are shown for completeness and we agree that they are not directly comparable to the ISSM results as the physics etc. differ in too many aspects. In the new version of the manuscript we have now better motivated and clarified our approach.

Minor Comments:

P1L2: ...'drives freshwater into the ocean'... State the explicit impact of this (e.g. undercutting at calving fronts?)
We updated this sentence and stated the impact.
P1L13-16 This paragraph would benefit from references.
We have added some references(Lliboutry, 1968; Röthlisberger, 1972 Gimbert et al. 2016).
P2L1: 'predominant in alpine glaciers and on the margins of the Greenland': This has more nuance, as channels develop seasonally, and are not predominant year round.
We added "and do usually develop over the summer season when a lot of melt water is available." in the sentence before.
P2L7: I think Hewitt (2013) should be mentioned here, as should Hoffman and Price (2014)

We have added the requested references.

P2L8: ...'remarkable results for spontaneously evolving channel networks'. The wording/concept could use clarification

Changed to "While these models demonstrate immense progress for modelling spontaneously evolving channel networks[...]".

P2L27-28: 'While the assumption ... with lower water input'. Citation needed

P3L15: hydraulic head needs a definition

We added "(water pressure in terms of water surface elevation above an~arbitrary datum; piezometric head)".

P3L18: Eq 2: porosity cancels itself out. Can you confirm that the units match up?

There was a typo in Eq. 2, missing a '+'. It should read $\rho_w \omega\, g\, (\beta_w + \frac{a}{w})$**.**

P3L19: the definition of alpha in table 1 reads the 'compressibility of water'. The definitions of alpha/beta_w in table 1 needs to be switched I think.

This is correct. We have corrected the mixup.

P3L25: although h is defined as the hydraulic head, it appears to be used as the saturated height

Yes, as soon as the aquifer becomes unconfined, the hydraulic head is the same as the saturated height.

P3L28: In Equation 5, it is unclear why Se(h) in the unconfined case depends on b. When the aquifer is unconfined (say with a saturated thickness of 1m), does it matter if the aquifer thickness is 10m or 20m? To gain a better overview of this formulation, I looked at the ' Groundwater flow equation' page on wikipedia (https://en.wikipedia.org/wiki/Groundwater_flow_equation). Although I admit that it is not an authoritative source, the formulation there states that Se(h) = S_s*b in the confined case, and S_e(h) = S'(h) is the unconfined case.

In the unconfined case, the storage is approximated by the specific yield S_y**, which is much larger than** $S_s b$ **(for the confined case). Therefore, adding a small term (**$S_s b$**) to a much larger term (**S_y**) does not really make a difference.**

P4Fig1: This should be updated/supplemented to show the physical interpretation of the models with channels.

We have updated the figure and added a colored section representing the efficient system. Together with the improved motivation it should be clear now, how to understand the representation with channels.

P5L17: I would move discretization to an appendix. It's beneficial to any reader looking to reimplement your model, but not necessary in the main text.

Done.

P7L16: Can you cite the upcoming results as Author(s) (In Prep)?

We will do so, as soon as the complete list of authors is known.

P8 Table 3: I think it would be beneficial to discuss these values compared to the inferred hydraulic conductivity values of till: 10^-9 - > 10^-4 m/s (Fountain and Walder, 1998).

Since we do not assume a till bed or any other specific type of drainage (as we hopefully made clearer now, see e.g. our answer to 13) in the first review), we don't think that we need this comparison.

P11L4: 'less' → 'lower'

Done.

P13L18: basal topography has no influence at all in the unconfined case?

Sorry, another typo, it should read "the confined-only solution completely depends on boundary conditions (apart from governing dK/dt)."

We added a seconds sentence to explain what we mean in more detail:

"The possibility of the aquifer to become unconfined captures the expected behaviour much better: At high water levels, water pressure distribution dominates water transport, while at low levels the bed topography becomes relevant."

P17L19: You need to define N_HUY.

Done.

P18L1: the quotient of X^-1 and Y^-1 could be simplified to the quotient of Y and X.

Yes, we have simplified that, see also 16) in the first review.

P18L8: It's important to add a citation here to MacAyeal (1989) and/or Morland (1987). In particular, the term SStA is confusing, since this approximation is often known as the SSA in the community. There is a proliferation of 'hybrid' models now, combining SSA and SIA, so a variation like SStA could be misinterpreted as one of those. I looked up the ISSM documentation to be sure that SStA was equivalent to SSA.

We agree that our term SStA is misleading as it is referenced as SSA in the corresponding ISSM documentation and references. However, if we are correct SSA is Shallow Shelf Approximation where the basal drag is zero. The Shelfy Stream Approximation (SStA) with the basal drag unequal zero is therefore different to the SSA. These terms are often mixed up in the literature. To be consistent with the ISSM documentation we now use the term SSA and give the corresponding citation.

P18L31: The improvement/comparison of your results should be quantified.

See our answer to 17) in the first review.

P19L8. 'This decisively illustrates the importance of having a real two-way coupling between the ice model and the basal hydrology model in order to obtain good results.' I don't believe you have shown this. You would have to show that you cannot reproduce the results with 2-way coupling, and then show that you reproduce the results when 2-way coupling is introduced. Since it is not cited, I would point the authors to Hoffman and Price (2014) for a detailed discussion on coupling of ice flow and subglacial hydrology.

In our opinion this constitutes another point in favour of including real two-way coupling. We agree that this is statement was a bit bold and we changed it accordingly in the manuscript.

P19L17: This sentence reads oddly.

Changed 'restitution' to 'decline'.

P24Fig10. The descriptions and panel labels are mixed up [there is no (d) in the figure caption]

We have added (d) to the caption.

A confined–unconfined aquifer model for subglacial hydrology and its application to the North East Greenland Ice Stream

Sebastian Beyer[1,2], Thomas Kleiner[2], Vadym Aizinger[2,3], Martin Rückamp[2], and Angelika Humbert[2,4]

[1]Potsdam Institute for Climate Impact Research, Potsdam, Germany
[2]Alfred Wegener Institute, Helmholtz Centre for Polar and Marine Research, Bremerhaven, Germany
[3]Friedrich–Alexander University Erlangen–Nürnberg, Erlangen, Germany
[4]University of Bremen, Bremen, Germany

Correspondence to: Sebastian Beyer (sebastian.beyer@awi.de)

Abstract. Subglacial hydrology plays an important role in the ice sheet dynamics as it determines the sliding velocity of ice sheets~~and~~. It also drives freshwater into the ocean, leading to undercutting of calving fronts by plumes. Modeling subglacial water has been a challenge for decades, and only recently new approaches have been developed such as representing subglacial channels and thin water sheets by separate layers of variable ~~permeability~~hydraulic conductivity. We extend this concept by modeling a confined and unconfined aquifer system (CUAS) in a single layer. The advantage of this formulation is that it prevents unphysical values of pressure at reasonable computational cost. We also performed sensitivity tests to investigate the effect of different model parameters. The strongest influence of model parameters was detected in terms governing the opening and closure of channels. Furthermore, we applied the model to the North East Greenland Ice Stream, where an efficient system independent of seasonal input was identified about $500\,\mathrm{km}$ downstream from the ice divide. Using the effective pressure from the hydrology model in the Ice Sheet System Model (ISSM) ~~shows~~ showed considerable improvements of modeled velocities in the coastal region.

1 Introduction

Subglacial water has been identified as a key component in glacial processes, it is fundamental in driving large ice flow variations over short time periods. Recent studies show considerable progress in modeling these subglacial networks and coupling them to ice models. Water pressure strongly influences basal sliding and can therefore be considered a fundamental control on ice velocity and ice-sheet dynamics (Lliboutry, 1968; Röthlisberger, 1972; Gimbert et al., 2016).

Generally, two fundamentally different types of drainage are identified: discrete channel / conduit systems and distributed water sheets or thin films. Distributed flow mechanisms are, for example, linked cavities (Lliboutry, 1968), flows through sediment/till (Hubbard et al., 1995), or thin water sheets (Weertman, 1957); those are considered to be an inefficient and slow system to transport water. Channels (Rothlisberger, 1969; Shreve, 1972; Nye, 1976) are seen as discrete single features or

arborescent networks; they usually develop over the summer season when a lot of melt water is available. It is assumed that these channelized or efficient drainage systems able to drain large amounts of water in short time spans are predominant in alpine glaciers and on the margins of Greenland, where substantial amounts of surface melt water are capable of reaching the bed (van den Broeke et al., 2017). In the interior of Greenland and also in most parts of Antarctica, the water supply is limited to melt due to the geothermal and frictional heating within the ice (Aschwanden et al., 2016) – a circumstance favoring distributed systems.

Seasonal variations of ice velocity have been observed and attributed to the evolution of the drainage system switching between an efficient and inefficient state in summer and winter (Bartholomew et al., 2010). For this reason, a new generation of subglacial drainage models has been developed recently that is capable of coupling the two regimes of drainage and reproducing the transition between them ~~(Schoof, 2010; Hewitt et al., 2012; Werder et al., 2013; De Fleurian et al., 2014)~~ (Schoof, 2010; Hewitt et al., 2012; Hewitt, 2013; Werder et al., 2013; De Fleurian et al., 2014; Hoffman and Price, 2014). While these models ~~produce remarkable results for~~ demonstrate immense progress for modeling spontaneously evolving channel networks, it is still a challenge to apply them on a continental scale. A comprehensive overview of the various ~~existing~~ operational and newly emerging glaciological hydrology models is given in Flowers (2015).

Distributed or sheet structures can naturally be well represented using a continuum approach, while channels usually require a secondary framework, where each feature is described explicitly. Water transport in channels is a complex mechanism that depends on the balance of melt and ice creep (Nye, 1976; Rothlisberger, 1969), channel geometry, and network topology. Additionally, the network evolves over time which further complicates modeling of this process. When simulating channel networks particular care must be also taken to prevent the emergence of instabilities due to runaway merging of channels (see the discussion in Schoof et al. (2012)). This leads to increased modeling complexity and high computational costs. An exception to this is the work of De Fleurian et al. (2014), where both systems are represented by Darcy flow through separate porous media layers. The layer representing the channels has its parameters (namely ~~permeability~~ hydraulic conductivity and storage) adjusted to exhibit the behavior of an effective system.

We take this idea even further and only use a single layer of Darcy flow with locally adjusted transmissivity of the layer at locations where channels form, while, at the same time, accounting for a decrease in storage. This means that we approximate the channel flow as a fast diffusion process similarly to work in De Fleurian et al. (2014); however, a single Darcy flow layer with spatially varying parameters (effective ~~permeability~~hydraulic conductivity) accounts for both drainage mechanisms. Similar approaches are known to have been applied to modeling of fracture networks in rock Van Siclen (2002). This reduced complexity model does not capture channels individually but represents their effect by changing specific local properties. Since our model aims to simultaneously represent the main properties of both drainage mechanisms (efficient and inefficient), special care must be exercised when choosing the model parameters and relating them to the physical properties of a specific scenario. While this strategy may not help to advance the precise understanding of channel formation processes, it captures the overall behavior and allows to examine the complex interactions on larger spatial and temporal scales. Currently we focus on channelised hydrology, whereas in future we will consider to expand the model towards cavity formation and closure. This is

primarily due to the fact that cavity formation is not considered a dominant effect underneath the large ice sheets (Fowler, 1987).

In addition, we introduce a new Confined–Unconfined Aquifer Scheme (CUAS) that differentiates between confined and unconfined flow in the aquifer (Ehlig and Halepaska, 1976). While the assumption of always saturated – and therefore confined – aquifers may be true for glaciers with large water supply, it does not hold in areas with lower water input. Especially in locations far from the coast, the water supplies are often insufficient to completely fill the aquifer. Ignoring this leads to significant errors in the computed hydraulic potential and unphysical, i.a. negative, water pressure. This problem has been analyzed in detail by Schoof et al. (2012), but here we study the effect in the context of equivalent aquifer models using unconfined flow as a possible solution.

Large scale ice flow models often compute the basal velocity using a Weertman-type sliding law, where the inverse of the effective pressure (difference between ice overburden pressure and water pressure) determines the velocity at the base. Low effective pressure leads to high basal velocity. Without subglacial hydrology models, the ice models simply take the ice overburden pressure as effective pressure completely neglecting water pressure. This is a major reason why these models struggle to represent fast flowing areas such as ice streams. The effective pressure computed by our model can be easily coupled to an ice sheet model and improve results for fast flowing areas.

The following work is structured as follows. In the next section, we present the one-layer model of subglacial aquifer and briefly describe its discretization. In Sect. 3 the model is applied to artificial scenarios, and the sensitivity to model parameters and stability are investigated. In addition, results for seasonal forcing are presented there, and we show how the model evolves over time. Section 4 demonstrates the first application of the proposed methodology to the North East Greenland Ice Stream (NEGIS), which is the only interior ice stream in Greenland. It penetrates far into the Greenland mainland with its onset close to the ice divide, so sliding apparently plays a major role in its dynamics. A short conclusions and outlook section wraps up the present study.

2 Methods

2.1 Confined–Unconfined Aquifer Scheme

The vertically integrated continuity equation in combination with Darcy's law leads to the general *groundwater flow equation* (see e.g. Kolditz et al. (2015)):

$$S\frac{\partial h}{\partial t} = \nabla \cdot (T\nabla h) + Q \tag{1}$$

with S the storage coefficient (change in the volume of ~~water released per unit decline~~ stored water per unit change of the hydraulic ~~potential~~ head over a unit area), h the hydraulic head (water pressure in terms of water surface elevation above an arbitrary datum; piezometric head), T transmissivity of the porous medium, and Q the source term. For a confined aquifer,

$T = Kb$, where K is the hydraulic conductivity, and b is the aquifer thickness. $S = S_s b$ with specific storage S_s given by

$$S_s = \rho_w \omega g \left(\beta_w + \frac{\alpha}{\omega} \right) \tag{2}$$

with material parameters for the porous medium (porosity ω, compressibility α) and water (density ρ_w, compressibility β_w).

~~Usually the transmissivity T is assumed as spatially uniform and isotropic, and the right hand side is written as $Kb\nabla^2 h + Q$.~~

In order to consider the general form covering both cases (confined and unconfined), we follow Ehlig and Halepaska (1976) and write the general form for the confined–unconfined problem:

$$S_e(h) \frac{\partial h}{\partial t} = \nabla \cdot (T(h) \nabla h) + Q. \tag{3}$$

Now the transmissivity and the storage coefficient depend on the head and are defined as

$$T(h) = \begin{cases} Kb, & h \geq b \quad \text{confined} \\ K\Psi, & 0 \leq h < b \quad \text{unconfined} \end{cases} \tag{4}$$

where $\Psi = h - z_b$ is the the local height of the head over bedrock z_b and effective storage coefficient S_e is given by

$$S_e(h) = S_s b + S'(h) \tag{5}$$

with

$$S'(h) = \begin{cases} 0, & b \leq \Psi \quad \text{confined,} \\ (S_y/d)(b - \Psi), & b - d \leq \Psi < b \quad \text{transition,} \\ S_y, & 0 \leq \Psi < b - d \quad \text{unconfined.} \end{cases} \tag{6}$$

This means that as soon as the head sinks below the aquifer height, the system becomes unconfined~~at this point~~, and therefore only the saturated section contributes to the transmissivity calculation. This also prevents the head from falling below the bedrock as detailed in Section 3.2. Additionally, the mechanism for water ~~release~~ storage changes from elastic relaxation of the aquifer (confined) to dewatering under the forces of gravity (unconfined). The amount of water ~~that is~~ released from dewatering is described by the specific yield S_y. Since ~~the amount of water released this way~~ this amount is usually orders of magnitudes larger than the release from confined aquifer ($S_y \gg S_s b$), it is useful to introduce a gradual transition as in Eq. (6) controlled by a user defined transition parameter d.

Note that the transmissivity is ~~no longer~~ not homogeneous making Eq. (3) nonlinear. This fits with our approach to describe the effective system (channels) by locally increasing the ~~permeability~~hydraulic conductivity. The benefit of this approach is discussed in Sect. 3.2.

Water pressure P_w and effective pressure N are related to hydraulic head as

$$P_w = (h - z_b)\Psi \rho_w g \tag{7}$$

and

$$N = P_\mathrm{i} - P_\mathrm{w} \tag{8}$$

with ~~z_b bedrock height,~~ g acceleration due to gravity, $P_\mathrm{i} = \rho_\mathrm{i} g H$ the cryostatic ice overburden pressure exerted by ice with thickness H and density ρ_i.

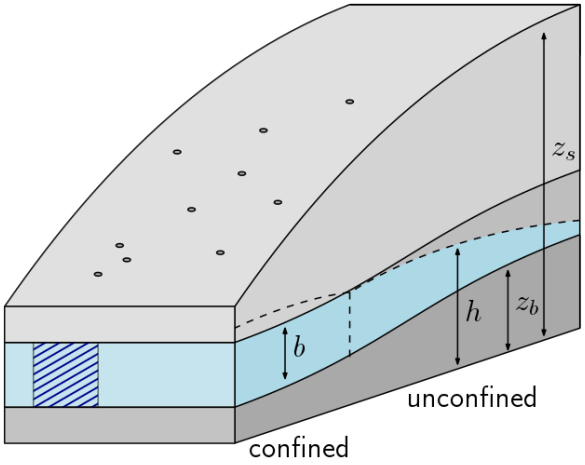

Figure 1. Schematics of the confined–unconfined aquifer scheme and artificial geometry for experiments. The hatched zone represents an area where the system is efficient. Dots on top indicate moulins.

2.2 Opening and closure

Opening and closure of channels is governed by melt at the walls due to the dissipation of heat and the pressure difference between the inside and outside of the channel leading to creep deformation. We follow de Fleurian et al. (2016) in using the classical channel equations from Nye (1976) and Röthlisberger (1972) to scale our transmissivity in order to reproduce this behavior. In contrast to de Fleurian et al. (2016), we do not evolve the aquifer thickness but the conductivity K, which leads to

$$\frac{\partial K}{\partial t} = v_\mathrm{melt} + v_\mathrm{creep}, \tag{9}$$

in which

$$v_\mathrm{melt} = \frac{r g \rho_\mathrm{w} b K}{\rho_\mathrm{i} L} \frac{r g \rho_\mathrm{w} \min(b, \Psi) K}{\rho_\mathrm{i} L} (\nabla h)^2 \tag{10}$$

and

$$v_\mathrm{creep} = 2 A n^{-n} |N|^{n-1} N K \tag{11}$$

with L the latent heat, r roughness factor, A the creep rate factor depending on temperature, and n the creep exponent, which we choose as $n = 3$. Depending on the sign of N, creep closure as well as creep opening can occur. Negative effective pressure over prolonged time is usually considered unphysical, and the correct solution to this would be to allow the ice to separate from the bed (see e.g. ~~(Schoof et al., 2012)~~ Schoof et al. (2012) for a possible solution). However, in the context of our equivalent layer model, Eq. (11) is still applicable because this is how a channel would behave for $N < 0$. In Sect. 3.1, we test the sensitivity of K and N to the magnitudes of r and A.

3 Experiments with artificial geometries

Testing out equivalent layer model and finding parameters for it is not straightforward because there are no directly comparable physical properties. Moreover, observations and measurements of subglacial processes are in general difficult and sparse. We address this by testing the model with some of the benchmark experiments of the **S**ubglacial **H**ydrology **M**odel **I**nter-comparison **P**roject (shmip.bitbucket.io).

The proposed artificial geometry mimics a land-terminating ice sheet margin measured $100\,\mathrm{km}$ in the x-direction and $20\,\mathrm{km}$ in the y-direction. The bedrock is flat ($z_b(x, y) = 0\,\mathrm{m}$) with the terminus located at $x = 0$ while the surface z_s is defined by a square root function $z_s(x, y) = 6\left((x + 5e3)^{1/2} - (5e3)^{1/2}\right) + 1$. Here, we use the SHMIP/B2 setup, which includes 10 moulins with ~~temporally constant~~ constant in time supply. Boundary conditions are set to zero influx at the interior boundaries ($y = 0$, $y = 20$, $x = 100$) and zero effective pressure at the terminus. All experiments start with initial conditions that imply zero effective pressure and are run for 50 years to ensure that they reach a steady state.

3.1 Parameter estimation and sensitivity

SHMIP is primarily intended as a qualitative comparison between different subglacial hydrology models, where results from the GlaDS model (Werder et al., 2013) serve as a "common ground". Here, we use it as a basis for an initial tuning and a study of the sensitivity of our model with regard to parameters. The upcoming results from the SHMIP are also the reason why we do not show a comparison to other models in this study but refer to the manuscript in preparation instead.

In Table 1, we show the physical constants ~~that we use~~ used in all setups and runs. The values in the lower half are properties of the porous medium and are only estimated. Since ~~we are dealing with them~~ they are utilized in the context of the equivalent layer model this is not an issue. Table 2 contains the model parameters in the upper part and the variables computed by the model in the lower part.

We divide the sensitivity analysis into a general block investigating the sensitivity to the amount of water input into moulins, the layer thickness b, the confined / unconfined transition parameter d, ~~model~~ grid resolution dx (Fig. 3) and a block that examines the parameters directly affecting channel evolution such as channel roughness factor r, creep rate factor A, and bounds for the allowed conductivity K_{min} and K_{max} (Fig. 5). In Table 3, we list values that lead to the best agreement with the SHMIP benchmark experiments and thus are used in the following as the baseline for our sensitivity tests.

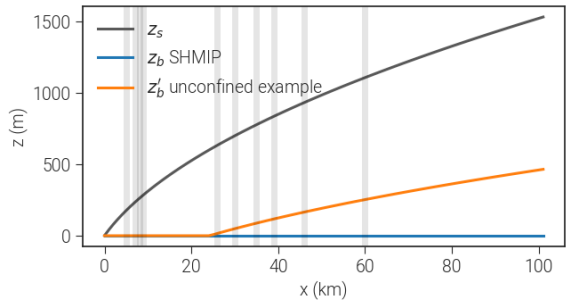

Figure 2. Experiments with artificial geometries. Vertical lines denote moulin positions for SHMIP/B2. The orange line shows the modified bedrock used to illustrate the impact of the confined/unconfined scheme as discussed in Sect. 3.2

Table 1. Physical constants used in the model. We distinguish between well known (upper half) and estimated / uncertain (lower half) parameters.

Name	Definition	Value	Units
L	latent heat of fusion	334	$\mathrm{kJ\,kg^{-1}}$
ρ_w	density of water	1000	$\mathrm{kg\,m^{-3}}$
ρ_i	density of ice	910	$\mathrm{kg\,m^{-3}}$
n	flow law exponent	3	-
g	gravitational acceleration	9.81	$\mathrm{m\,s^{-2}}$
~~α~~ β_w	compressibility of water [a]	~~10^{-8}~~ 5.04×10^{-10}	$\mathrm{Pa^{-1}}$
~~β_w~~ α	compressibility of porous medium[a]	~~5.04×10^{-10}~~ 10^{-8}	$\mathrm{Pa^{-1}}$
ω	porosity[a]	0.4	-
S_s	specific storage (Eq. (5))	$\approx 1 \times 10^{-4}$	$\mathrm{m^{-1}}$
S_y	specific yield	0.4	

[a] Values from De Fleurian et al. (2014)

In Figs. 3a and b, the model's reaction to different amounts of water input through the moulins is shown. With deactivated conductivity evolution ($K = \mathrm{const.}$, dashed lines), larger water inputs lead to higher water pressure, hence lower effective pressure N. In this case, a moulin input of $18\,\mathrm{m^3\,s^{-1}}$ leads to negative values of N. With activated evolution of K, the conductivity adapts to the water input: as more water enters the system through moulins, the conductivity rises. Vertical gray bars show the location of moulins along the x-axis, and the most significant increase in K occurs directly downstream of a moulin. This happens because the water is transported in this direction leading to increased melt. At the glacier snout ($x = 0$), the ice thickness is at its lowest so almost no creep closure takes place; hence, the conductivity reaches its allowed maximum of $0.5\,\mathrm{ms^{-1}}$ for all tested parameter combinations. Significant development of effective drainage is visible for inputs above

Table 2. Model parameters (upper) and variables computed in the model (lower)

Name	Definition	Units
$K_{\min}$	min. conductivity	$\mathrm{m\,s^{-1}}$
$K_{\max}$	max. conductivity	$\mathrm{m\,s^{-1}}$
b	aquifer thickness	m
d	confined / unconfined transition (Eq. (6))	m
Q	water supply	$\mathrm{m\,s^{-1}}$
r	roughness factor	-
A	creep rate factor	$\mathrm{Pa^{-3}\,s^{-1}}$
h	hydraulic head	m
K	hydraulic conductivity	$\mathrm{m\,s^{-1}}$
S	storage	-
S_e	effective storage	-
T	transmissivity	$\mathrm{m^2\,s^{-1}}$
v_{melt}	opening by melt	$\mathrm{m\,s^{-2}}$
v_{creep}	opening/closure by creep	$\mathrm{m^{-2}}$
P_{w}	Water pressure	Pa
P_{i}	Ice pressure	Pa
N	effective pressure	Pa

Table 3. Selected baseline parameters for all experiments unless otherwise noted. These parameters best match the SHMIP targets.

Name	Value	Units
$K_{\min}$	0.003	$\mathrm{m\,s^{-1}}$
$K_{\max}$	0.5	$\mathrm{m\,s^{-1}}$
b	10	m
d	0	m
dx	1000	m
r	1	-
A	5×10^{-25}	$\mathrm{Pa^{-3}\,s^{-1}}$
$Q_{\mathrm{per\ moulin}}$	9	$\mathrm{m^3\,s^{-1}}$

$2.25\,\mathrm{m^3 s^{-1}}$ (yellow line). The resulting effective pressure decreases with rising water input as the system becomes more efficient at removing water. Up to ca. $35\,\mathrm{km}$ distance from the snout this results in almost identical values of N for all forcings above $2.25\,\mathrm{m^3\,s^{-1}}$. The system adapts so that it can remove all of the additional water efficiently. In Figs. 3i and j, the two-

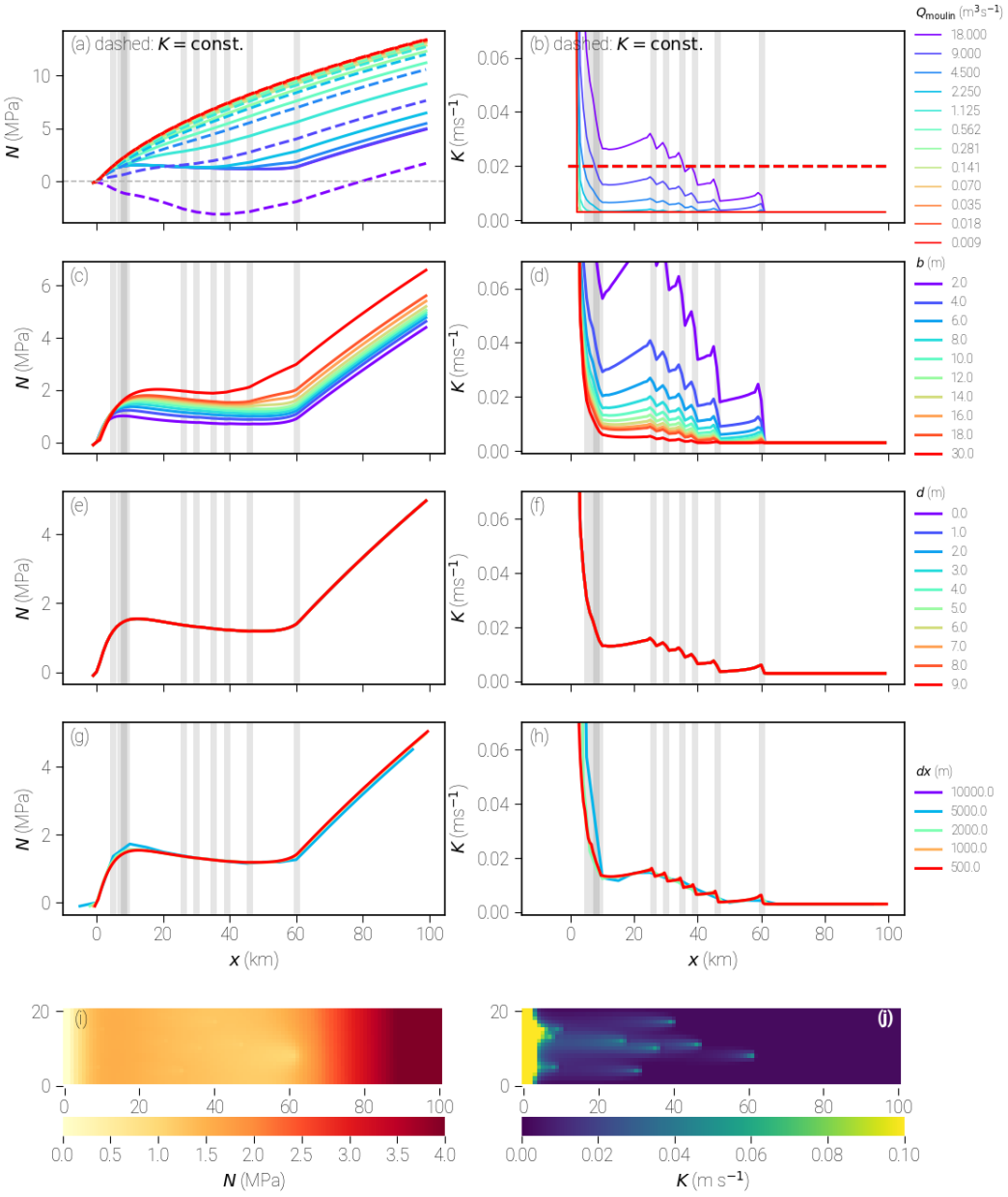

Figure 3. Results from the general sensitivity experiments showing the dependence of N (left) and K (right) on: (a)–(b) Water supply from moulins Q_{moulin} (results for deactivated conductivity evolution are shown using dashed lines), (c)–(d) aquifer layer thickness b, (e)–(f) confined/unconfined transition parameter d, (g)–(h) ~~model~~ grid resolution dx. Shown values are averaged along the y-axis to represent cross sections at flow lines. Conductivity plots are cut off at $0.06\,\mathrm{ms}^{-1}$ to improve visibility of the relevant range. (i) and (j) show the two-dimensional distributions (map view) of the results using the best-fit baseline parameters.

dimensional distributions of N and K are shown for the baseline parameters; in addition, we detail the temporal development of K in Fig. 4.

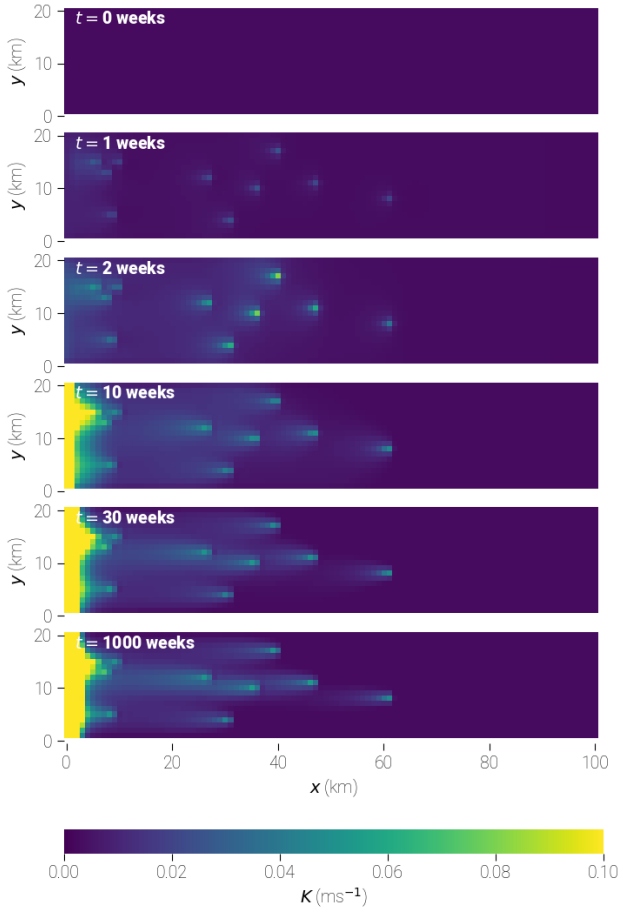

Figure 4. Development of conductivity over time

"Channels" (indicated by regions of high conductivity) form downstream from moulins and continue straight towards the ocean. The effective pressure drops around water inputs and along the ~~channels. We detect small fluctuations in K directly downstream of moulins ("checkerboard patterns") (Figs. 3j and 4); we attribute them to the effects of high conductivity "channels"(giving rise, in turn, to high head gradients that causes aliasing on rather coarse grids used in our simulations). This finding is motivated by the following observations: no fluctuations are seen in the channel corresponding to the rightmost moulin – same as in the results for a single moulin not shown here, the amplitude of fluctuations decreases rapidly with increasing grid resolution (Fig. 3h). In addition, the fluctuations appear to have no significant effect on the resulting pressure distribution.~~ "channels".

The layer thickness b directly influences the transmissivity according to Eq. (4). A thicker layer can transport more water out of the system and therefore leads to ~~less~~ lower water pressure and higher effective pressure (Figs. 3c and d). At the same time, a thinner layer leads to increased water pressure and higher pressure gradients which results in higher v_{melt} and can induce negative effective pressure and creep opening.

The confined–unconfined transition parameter d does not show noticeable effects on the results (Figs. 3e and f) because the experiment has sufficient water input so that all cells are confined in the steady state.

Grid resolution dx has low influence on the pressure distribution ~~but a large~~ and a minor effect on the conductivity downstream (Figs. 3g and h). ~~Coarse resolutions lead to large spatial fluctuations of K. Fine resolutions show a weaker checkerboard pattern, which supports our assumption that the pattern results from large gradients in the hydraulic head~~However, coarse resolutions are unable to resolve the steps that appear at the moulins.

In Figs. 5a and b, we show the results for different values of K_{min}. K_{min} ensures that the system is never completely watertight and determines how much water can pass through independently of the system's current state. Higher values lead to more water transport, lower water pressure, and higher effective pressure. In this experiment, values higher than $0.01\,\mathrm{m\,s^{-1}}$ show no reactions of K to moulins upstream of $10\,\mathrm{km}$.

K_{max} (Fig. 5e and f) has no visible impact on the resulting pressure distribution. The differences in K are only large at the snout, where the maximum is always reached because the ice thickness is too low to counteract the melt term. No significant influence on the upstream area has been detected. ~~Rises in conductivity downstream of moulins are amplified with larger K_{max}.~~

The creep rate factor A determines the "softness" of the ice and therefore effects the creep term in Eq. (9). Larger values of A imply warmer ice; hence, more creep closure (see Figs. 5e and f). Note, that this also effects creep opening if $N < 0$.

The roughness factor r is meant as a measure for small bumps and imperfections, where a rougher ~~channel~~ "channel" (larger r) would ~~endure~~ experience more melt because of the larger contact area and more turbulent mixing. Larger values of r lead to higher conductivity and more water transport resulting in lower P_{w} and higher N.

3.2 The benefit from treating unconfined aquifer

As described above, the confined–unconfined aquifer approach is advantageous ~~in~~ for obtaining physically meaningful pressure distributions. In the example illustrated in Fig. 6, we use a slightly modified geometry, where the bedrock rises towards the upstream boundary forming a slab $z_b'(x,y) = \max\left(3((x+5e3)^{1/2} - (5e3)^{1/2}) - 300, 0\right)$. The supply is constant in time and space, and we choose a low value of 7.93e-11 m/s (≈2.5 mm/a) to compare our improved scheme to the simple confined only case. Fig. 6 shows a comparison of the steady state solutions: For the confined-only case, the hydraulic head drops below the bedrock at the upstream region. This results in negative water pressure for these regions. Addressing this by simply limiting the water pressure to zero would result in inconsistencies between the pressure field and the water supply. Our new scheme limits the transmissivity when the head approaches the bedrock and by this means ensures $p_w \geq 0$ in a physically consistent way. Additionally, the ~~unconfined-only~~ confined-only solution completely depends on boundary conditions and supply terms, basal topography has no influence in this case ~~.~~ (apart from governing dK/dt). The possibility of the aquifer to become unconfined

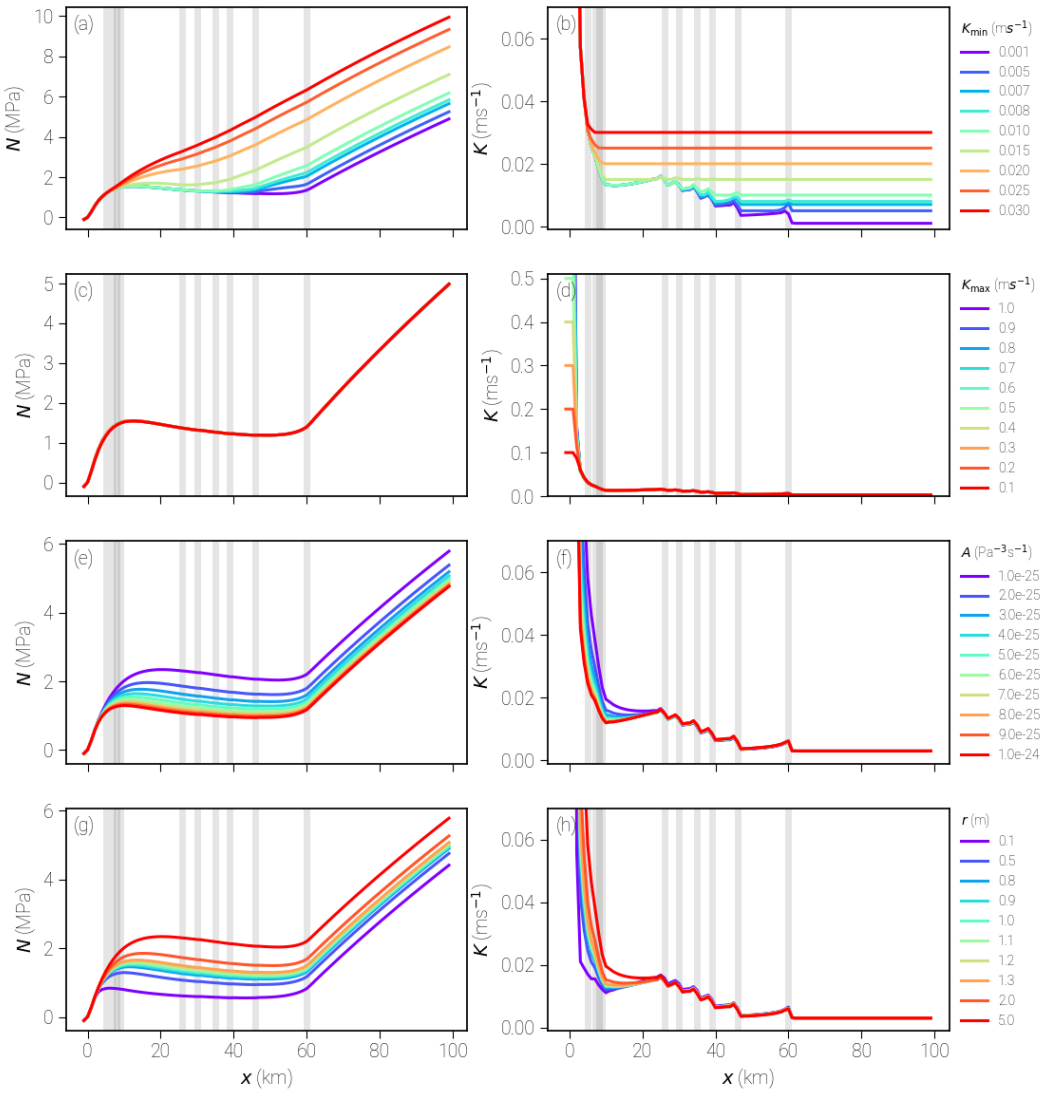

Figure 5. Results from parameters directly related to opening and closure: Limits on the conductivity $K_{\min}$ (panels a and b) and $K_{\max}$ (panels c and d), creep rate factor A (panels e and f) and roughness factor r (panels g and h). Shown values are averaged along the y-axis to represent cross sections at flow lines. Conductivity plots are cut off at $0.06\,\mathrm{ms}^{-1}$ to improve visibility of the relevant range.

captures the expected behaviour much better: At high water levels, water pressure distribution dominates water transport, while at low levels the bed topography becomes relevant.

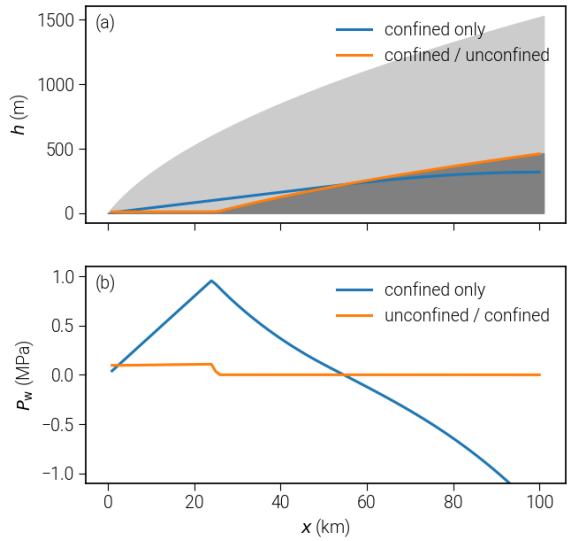

Figure 6. Advantages of using the confined/unconfined aquifer scheme (CUAS): Values of head and water pressure for geometries with non-flat bedrock. (a) Computed head for the confined and combined scheme with ice geometry in the background. In the confined only case, the head ~~is~~ goes below bedrock. (b) Resulting water pressure, only for the combined scheme the pressure is always non-negative.

3.3 Seasonal channel evolution and properties

In order to understand our model's ability to simulate the seasonal evolution of subglacial systems, we selected the setup SHMIP/D and ran it with different values of key model parameters. This experiment does not include any moulins but prescribes a non-uniform spatial distribution of supply instead that also varies seasonally. A simple degree day model with varying temperature parameter $d\Theta$ provides water input rising from the downstream end (lowest elevated) of the glacier towards the higher elevated areas over summer:

$$\Theta(t) = -16\cos(2\pi/\mathrm{yr}\, t) - 5 + d\Theta \tag{12}$$

$$Q_{\mathrm{dist}}(z_s, t) = \max(0, (z_s \mathrm{LR} + \Theta(t))\mathrm{DDF}) + Q_{\mathrm{basal}}. \tag{13}$$

Here, $\mathrm{yr} = 31536000\,\mathrm{s}$ denotes the number of seconds per year, $\mathrm{LR} = -0.0075\,\mathrm{Km}^{-1}$ the lapse rate, $\mathrm{DDF} = 0.01/86400\,\mathrm{mK}^{-1}\mathrm{s}^{-1}$ is the degree day factor, and $Q_{basal} = 7.93 \times 10^{-11}\,\mathrm{ms}^{-1}$ is additional basal melt. The resulting seasonal evolution of the supply is shown in Fig.7a. The model is run for 10 years so that a periodic evolution of the hydraulic forcing is generated. Here, we present the result for one parameter set only since the model is not very sensitive in this setup. For the prescribed water supplies, the conductivity only reaches its lower limit K_{min} for very short periods, and the upper limit K_{max} is never reached at all (apart from the terminus, where it does not have any significant influence on the upstream behavior of the system as we have shown in the previous experiment).

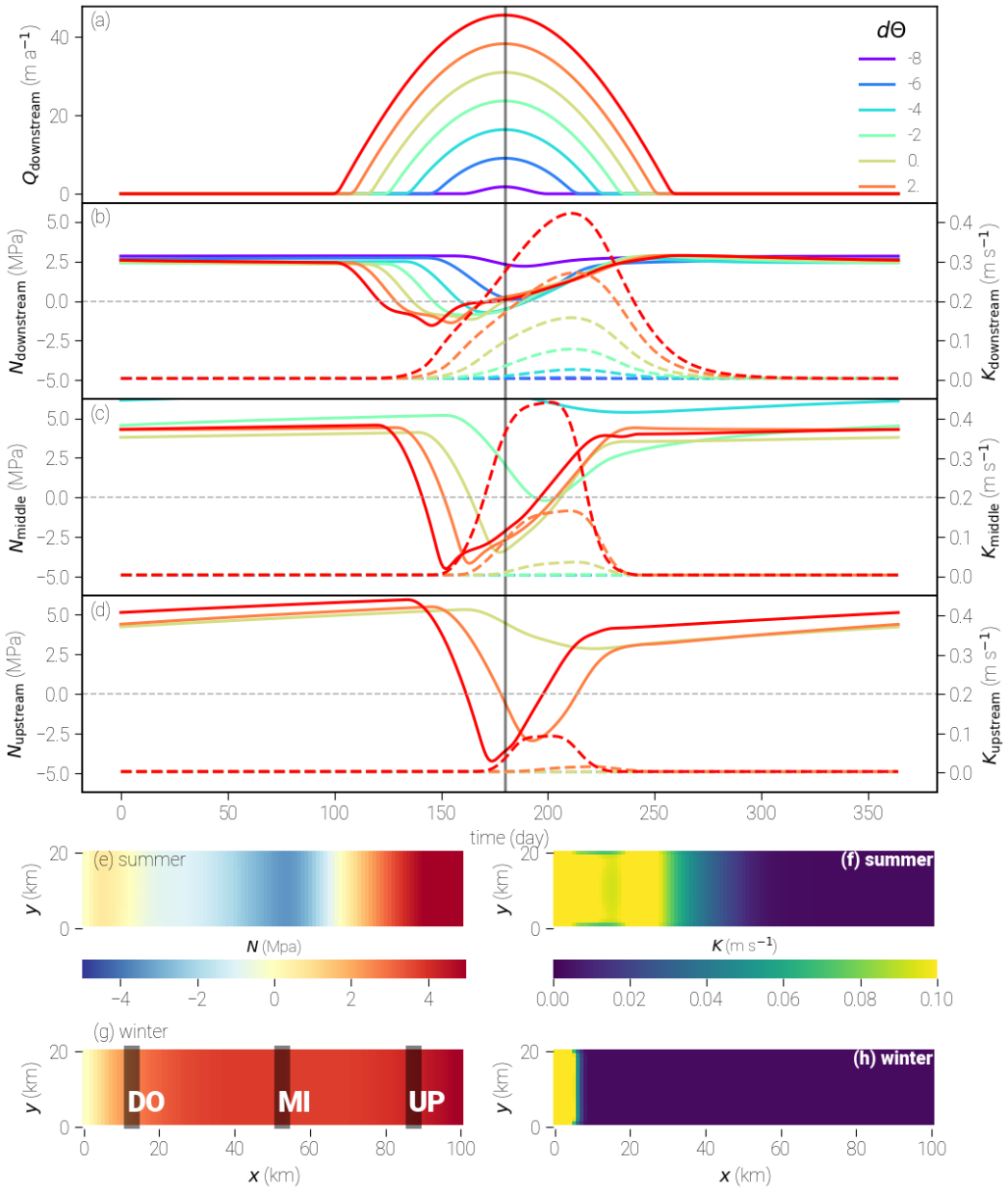

Figure 7. Results for one season of the SHMIP/D experiment. In panels (b)–(d), the left axis (effective pressure) corresponds to the solid lines, while the right axis (conductivity) specifies the values for the dashed lines. The values at the given positions (upstream, middle, downstream) are averaged over the corresponding areas indicated in panel (g). Panels (e)–(h) show two-dimensional distribution maps of $d\Theta = 0$ runs.

We chose three different locations to present N and K during the season: downstream of the glacier close to the snout, in the center, and at a far upstream location (Figs. 7b–d; the locations are marked in panel g). Shown time series are spatially averaged over these locations with solid lines representing the effective pressure and dashed lines the conductivity.

Water input increases during the summer months, while the corresponding effective pressure drops. With a time lag the conductivity rises in response. Supply develops from downstream towards the upstream end of the glacier over the season so the decline in N at the downstream location (Fig. 7b) is instantaneous when the supply rises, while at the further inland locations (Figs. 7c and d) N reacts later during the year. At the middle location, the drop in N is more intense almost reaching $-5\,\mathrm{MPa}$ for the temperature parameters of 2 and higher. Temperature parameters below -4 show no response at this location. The same applies to the change in conductivity: only the three highest temperatures lead to a significant rise of K. Finally, at the upstream position, only for $d\Theta = 4$ and $d\Theta = 2$ the effective pressure drops below zero, while for $d\Theta = 0$ the drop is smaller in magnitude and more prolonged. ~~Conductivity~~ The conductivity rise is only significant for $d\Theta = 4$ at this location. While the onset and minima of the decline in N strongly depend on the amount and timing of the water input for all values of $d\Theta$, the maximum of K and also the time when N returns to winter conditions is similar. For the downstream position, the maximum conductivity is reached for day 210, and N reaches its background value approximately 25 days later. At the center and upstream positions, this behavior is less pronounced but generally similar.

The observed behavior is expected and indicates that our model is able to represent the seasonal evolution of the subglacial water system. Increasing water supply over the year leads to rising water pressure and dropping effective pressure. When the conductivity rises in response, the effective pressure goes up again despite the supply not yet falling again because the more efficient system is able to transport the water away. For the cases, where no visible change in K occurs such as $d\Theta = -6$ (blue line in Fig. 7b), the effective pressure directly follows the supply at the terminus, while at the center position ($d\Theta = -2$, cyan line, Fig. 7c), the minimum is offset by the time needed for the supply to reach that location. The maximum in conductivity K is reached later because once the system ~~gets~~ becomes efficient, increased water transport stimulates melting that opens the system even more. This self-reinforcing process is only stopped when enough water is removed and the reduced water flux reduces the melt again. We assume that this leads to similar locations of the conductivity maxima for different $d\Theta$ and the resulting similar reemerging of winter conditions in N.

In this experiment, N becomes negative during the seasonal evolution, which is not physically meaningful. We attribute such behavior to a lack of adjustment of water supply to the state of the system. In reality, the supply from runoff or supraglacial drainage would cease as soon as the pressure in the subglacial water system becomes too high; here we simply continue to pump water into the subglacial system without any feedback. This then leads to negative values of N. It is also consistent with the finding that N becomes negative earlier in the season in cases of higher supply. This deficiency will be addressed in future work.

4 Subglacial hydrology of NEGIS, Greenland

The role of subglacial hydrology in the genesis of ice streams in general is not well understood yet. NEGIS is a very distinct feature of the ice sheet dynamics in Greenland; thus, the question about the role of subglacial water in the genesis of NEGIS is critical. The characteristic increase in horizontal velocities becomes apparent about $100\,\mathrm{km}$ downstream from the ice divide (Vallelonga et al., 2014). Further downstream, the ice stream splits into three different branches: the 79° North Glacier (79NG),

Zacharias Isbrae (ZI), and Storstrømmen. Thus far, large scale ice models have only been able to capture the distinct flow pattern of NEGIS when using data assimilation techniques such as inverting for the basal friction coefficient (see e.g. horizontal velocity fields in Goelzer et al., 2017). It is assumed that most of the surface velocity can be attributed to basal sliding amplified by basal water instead of ice deformation (Joughin et al., 2001). This means that the addition of a subglacial hydrology might have the potential to improve the results considerably. While many glaciers in Greenland have regularly draining supraglacial lakes and run-off driving a seasonality of the flow velocities, little is known about the effect at NEGIS (Hill et al., 2017). Because of this lack of data, to avoid an increased complexity, and to focus on the question if basal melt alone can account for the development of an efficient system, we do not include any seasonal forcing into our experiment.

Our setup includes the major parts of this system. The pressure adjusted basal temperature Θ_{pmp} obtained from PISM (Aschwanden et al., 2016) is utilized to define the modeling region. We assume that for freezing conditions at the base ($T_{\mathrm{pmp}} < 0.1\,\mathrm{K}$) basal water transport is inhibited and take this as the outline of our model domain. Fig. 8 shows the selected area and PISM basal melt rates used as forcing.

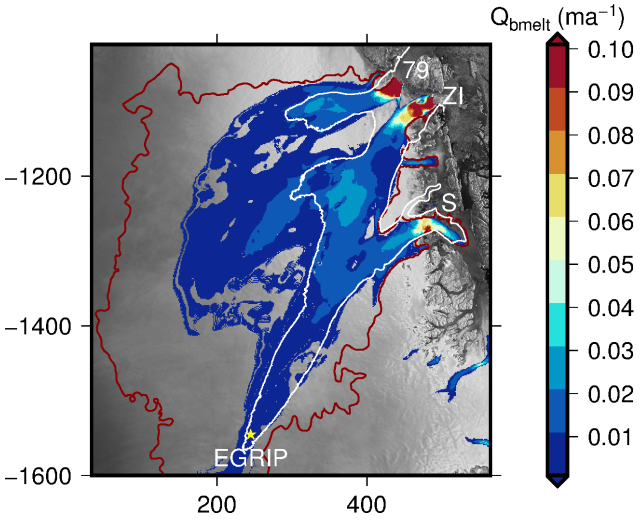

Figure 8. Boundary conditions and forcing for NEGIS experiment. Shown is the basal melt rate from PISM and contour line for $\Theta_{\mathrm{pmp}} = -0.1\,\mathrm{K}$ ~~, which is~~ (red) used as model boundary~~, in red~~.

For the ice geometry, we use the ~~data~~ bed model of Morlighem et al. (2014) interpolated on a 1.2 km grid. Boundary conditions at lateral margins are set to no flux, whereas the termini at grounding lines are defined as Dirichlet boundaries with a prescribed head that implies an effective pressure of zero. This means that the water pressure at the terminus is equal to the hydrostatic water pressure of the ocean assuming floating condition for the ice at the grounding line. Parameters used for this experiment are the same as those for the previous experiments (Table 3) but with K_{max} reduced to $0.3\,\mathrm{ms}^{-1}$ to speed up the computation. The experiment is run for 50 a to reach steady state. Despite the large number of cells (444×481), computing time for this setup is still reasonable (48 hours on a single core of Intel Xeon Broadwell E5-2697).

The resulting distributions of effective pressure and conductivity are shown in Figs. 9a and b, respectively. As expected, effective pressure is highest at the ice divide and decreases towards the glacier termini. Conductivity is low for the majority of the study area with the exception of areas in the vicinity of grounding lines and two distinct areas that touch in between 79NG and ZI. The northern area (marked I in Fig. 9b) is located at the northern branch of 79NG and has no direct connection to the snout. The second area (marked II in Fig. 9b) emerges in the transition zone between the southern branch of 79NG and Zacharias Isbrae and covers an area approximately twice as large as area I with higher values of K. It is connected to the snout of ZI with narrow band of high conductivity cells.

Comparing the effective pressure distribution to the observed velocity (Rignot and Mouginot, 2012) – we chose the $50\,\mathrm{m\,a^{-1}}$ contour line as indicator of fast flow – we observe ~~coincidence of~~ a high degree of overlap between the fast flowing ~~areas~~ regions and those with low effective pressure (below $1\,\mathrm{MPa}$) over most of the downstream ~~areas in~~ domain of our study area. Storstrømmen shows slightly higher effective pressure than 79NG and ZI, which is in accordance with lower observed horizontal velocities for that glacier (Joughin et al., 2010). At the onset of the NEGIS, the effective pressure is high, and no relationship to the flow velocity can be observed.

To further examine the possible influence of our hydrology model to basal sliding~~we look at~~, we investigate the impact on the sliding law. ~~Usually the effective pressure is assumed to simply be~~ We chose to compare our computed N_{CUAS} to the reduced ice overburden pressure ~~N_{HUY} (Huybrechts, 1990). Therefore, we~~, defined in Huybrechts (1990) as $N_{\mathrm{HUY}} = P_{\mathrm{i}} + \rho_{\mathrm{sw}} g (z_b - z_{\mathrm{sl}})$ for $z_b < z_{\mathrm{sl}}$ and $N_{\mathrm{HUY}} = P_{\mathrm{i}}$ otherwise.

We show the quotient of ~~the inverse of effective pressure in CUAS N^{-1}_{CUAS} and H^{-1}_{HUY}~~ H_{HUY} and N_{CUAS} in Fig. 9c. This demonstrates where the application of our hydrology model would increase basal velocities.

In order to demonstrate the effect of the modeled subglacial hydrology system on the NEGIS ice flow, we setup a simple, one-way coupling to an ice flow model. Here, we use the Ice Sheet System Model (ISSM, Larour et al., 2012), an open source finite element flow model appropriate for continental scale and outlet glacier applications (Bondzio et al., 2017; Morlighem et al., 2016). The modeling domain covers the grounded part of the whole NEGIS drainage basin. The ice flow is approximated with the ~~Shelfy-Stream Approximation (SStA)~~ Shallow Ice Approximation (SSA, MacAyeal, 1989; Morland, 1987) within a 2D plan-view model, which is appropriate for fast flowing ice ~~.~~ but not for the slow flowing parts in our model area. Since we aim do demonstrate that our addition of the hydrology model improves results in fast flowing areas where the SSA is valid, this is not a huge concern. As we use the ~~SStA~~ SSA we do not perform a thermo-mechanical coupling but prescribe a depth-averaged hardness factor in Glens flow law. Model calculations are performed on an unstructured finite element grid with a high resolution of $1\,\mathrm{km}$ in fast flow regions and coarse resolution of $20\,\mathrm{km}$ in the interior. The basal drag $\boldsymbol{\tau}_b$ is written in a Coulomb-like friction law:

$$\boldsymbol{\tau}_b = -k^2 N \mathbf{v}_b, \tag{14}$$

where $\mathbf{v}_b$ is the basal velocity vector tangential to the glacier base, N the effective pressure, and k^2 a positive constant. We run two different scenarios, where (1) the effective pressure is parametrized as the reduced ice overburden pressure, $N = N_{\mathrm{HUY}}$, and (2) the effective pressure distribution is taken from the hydrological model at steady state, $N = N_{\mathrm{CUAS}}$. The value of k^2

is tuned in order to have ice velocities of approximately $1500\,\mathrm{m\,a^{-1}}$ at the grounding line at the 79NG. For both scenarios, the value of k^2 is $0.1\,\mathrm{s\,m^{-1}}$. The results for both scenarios are shown in Fig. 10a and c, respectively. Additionally, we show the observed velocities (Fig. 10d, Rignot and Mouginot, 2012) and the PISM surface velocities (Fig. 10b, Aschwanden et al., 2016). Note that the latter is a PISM model output on a regular grid interpolated to the unstructured ISSM grid.

Velocities computed with the reduced ice overburden pressure are generally too slow and do not resemble the structure of the fast flowing branches at all. The result from PISM shows distinct branches for the different glaciers, which display a relatively sharp separation from the surrounding area. Note, that PISM also uses a basal hydrology model as described in Bueler and van Pelt (2015). Velocities are slightly lower than observed velocities, especially for Zacharias Isbrae and in the area, where ZI and 79NG are closest. In the upper part towards the ice divide, the ice stream structure is not visible in the velocities. The ISSM model using effective pressure computed by CUAS produces high velocities towards the ocean that closely resemble N. The transition between the ice streams and the surrounding ice is poorly reproduced. While the stream structure is way too diffused, the velocity magnitude for the glaciers appears reasonable. The inland part is similar to observed velocities but – as in the PISM simulation – the upper part where NEGIS is initiated is not present. The onset of NEGIS is thought to be controlled by high local anomalies in the geothermal flux (Fahnestock et al., 2001), which PISM currently does not account for. Higher geothermal flux would lead to more basal melt, hence, water supply in the hydrology model. However, the consequences for the modeled effective pressure would require further experiments which are not in the scope of this paper.

In Tab. 4 we show the root mean square error ($l2$ -norm), Pearson correlation coefficient r^1 and Δv ($l1$ -norm) between the modeled and observed velocities.

Table 4. Comparison of modeling results for ice velocity to observed values (Rignot and Mouginot, 2012). Herein RMS denotes the root mean square error or $l2$ -norm, r^2 is the Pearson correlation coefficient and ΔV is the $l1$ -norm.

	RMS ($\mathrm{m\,a^{-1}}$)	r^2	Δv ($\mathrm{m\,a^{-1}}$)
ISSM with reduced ice overburden pressure	176.83	0.69	90.13
PISM (Aschwanden et al., 2016)	132.05	0.84	65.42
ISSM with N computed from CUAS	126.86	0.80	53.28

We find it impressive that even without extensive tuning, we can considerably improve the velocity field in ISSM by our simple one-way coupling to the hydrology model. However, the results in this section are to be understood not as a thorough study of the NEGIS ~~,~~ but as a first application of the model to a real geometry. A complete study requires extended observations in order to determine the optimal model parameters. However, we are confident that our results represent the general aspects of the hydrological system at NEGIS. Based on our sensitivity and seasonal experiments (Sect. 3.1 and Sect. 3.3) we expect the high-conductivity-areas to be a stable feature, which would extend or retract depending on the chosen values of the melt and creep parametrizations but not change their location. Available supply plays a more important role here, and we assume that different basal melt distributions – or the addition of surface melt – might considerably change the position and the extent of the efficient system and, therefore, the effective pressure distribution as ~~we~~ can be seen in Sect. 3.3.

The onset of NEGIS is not well reproduced in the PISM simulation as well as in our ISSM result. Since the ice is slow in the PISM results in that area, basal melt rates are low, and, since we use these as input in our hydrology model, it is expected that our model computes low water pressure here. ~~This decisively illustrates the importance~~ In our opinion this another point of having a real two-way coupling between the ice model and the basal hydrology model in order to obtain good results. These results could then in turn be used to guide further optimization of the modeling parameters in our hydrology model in the future.

5 Conclusions

We present the first equivalent aquifer layer model for subglacial hydrology that includes the treatment of unconfined water flow. It uses only a single water layer with adaptive conductivity. Since extensive observations of the subglacial system are rare, its relative simplicity and empirical nature can be an advantage.

We find strong model sensitivity to the lower limit of conductivity $K_{\min}$, grid spacing dx, and the parametrization of melt v_{melt} and creep v_{creep}, while the sensitivity to the upper limit of conductivity $K_{\max}$ and the confined–unconfined transition parameter d is low. Our model robustly reproduces the seasonal cycle with the development and ~~restitution~~ decline of the effective system over the year. Another positive aspect of our modeling approach was the complete absence of instabilities similar to those arising due to runaway channel enlagement – even at high flow rates. We attribute this fact that our combined confined/unconfined aquifer model quickly transports excess water away from confined aquifer parts, where high water pressure could lead to steep increases in effective conductivity (via negativ v_{creep} term).

In our NEGIS experiments, we find the presence of a partial efficient system for winter conditions. The distribution of effective pressure broadly agrees with observed velocities, while the upstream part is not represented correctly. When coupled to ISSM, our hydrology model notably improves computed velocities.

A number of aspects of the proposed model can be further developed; those include improved parametrizations of several physical mechanisms (e.g. adding feedback ~~for~~ between pressure and water supplies), changing ~~scalar conductivity (and thus also the permeability)~~ the hydraulic conductivity coefficient to a ~~tensor~~ tensor-valued on to better represent the ~~channel anisotropy~~ anisotropy of channel networks, and, last but not least, transition to a mixed formulation of the Darcy equation discretized on an unstructured mesh in order to preserve mass conservation and ~~improve computational efficiency~~to improve resolution in the areas of interest.

Appendix A: Parametrization of evolution of conductivity

We use the same parametrization as de Fleurian et al. (2016) detailed here using the notation in Cuffey and Paterson (2010).

Creep term

Nye (1976), found for the closure on channels due to creep that

$$\frac{1}{R_c}\frac{\partial R_c}{\partial t} = A\left[\frac{N}{n}\right]^n, \tag{A1}$$

with R_c denoting the channel radius and A_c the channel area ($=\pi R_c^2$) (notation as in (Cuffey and Paterson, 2010, Eq. 6.15)).

Multiplication by $2\pi\rho_i R_c^2 = 2\rho_i A_c$ on both sides, leads to

$$2\pi\rho_i R_c\frac{\partial R_c}{\partial t} = 2\rho_i A_c A\left[\frac{N}{n}\right]^n \tag{A2}$$

Rewriting the left side to area, using the chain rule ($\frac{\partial A_c}{\partial t} = 2\pi\frac{\partial R_c}{\partial t}$) yields

$$\rho_i\frac{\partial A_c}{\partial t} = 2\rho_i A_c A\left[\frac{N}{n}\right]^n. \tag{A3}$$

Melt term

Heat produced over ds in unit time is $Q_w G$ and pressure melting point effects are $\rho_w Q_w c_w \mathcal{B}\frac{dP_i}{ds}$, which leads to

$$\dot{M}L_f = \underbrace{Q_w G}_{\text{turb. heat produced}} \underbrace{-\rho_w Q_w c_w B\frac{dP_i}{ds}}_{\text{PMP effect}} \tag{A4}$$

(Cuffey and Paterson, 2010, Eq. 6.16), where $\dot{M}$ represents the melt rate (mass per unit length of wall in unit time) and the magnitude of gradient of the hydraulic potential is given by

$$G = |\nabla\phi_h|, \quad \text{where} \quad \phi_h = \rho_w g h. \tag{A5}$$

Neglecting the PMP effects we get

$$\dot{M} = \frac{Q_w G}{L_f} \tag{A6}$$

using $Q_w = qb$ (confined case, unconfined would be $Q_w = q(h - z_b)$) and $q = K\nabla(h)$ (ommiting the minus, because we need the magnitude here) this is

$$\dot{M} = \frac{K\nabla(h)b\nabla(\rho_w g h)}{L_f} \tag{A7}$$

which can be rewritten to

$$\dot{M} = \frac{\rho_w g K b(\nabla h)^2}{L_f}. \tag{A8}$$

Opening and closure

The conduit expands when there is more melt than ice inflow due to creep

$$\rho_i \frac{\partial A_c}{\partial t} = \dot{M} - \underbrace{2\rho_i A_c A \left[\frac{N}{n}\right]^n}_{\text{creep term from A3}} \tag{A9}$$

(Cuffey and Paterson, 2010, Eq. 6.42). Inserting $\dot{M}$ from Eq. A8 and dividing by ρ_i results in

$$\frac{\partial A_c}{\partial t} = \frac{\rho_w g K b (\nabla h)^2}{L_f \rho_i} - 2 A_c A \left[\frac{N}{n}\right]^n. \tag{A10}$$

Change of area to conductivity

This is a purely geometrical argument, since we are interested in the transmissivity $T = Kb$ ($T = Kh$ for unconfined) and therefore, a change in K is equivalent to a change in the aquifer thickness b .

Hence, we add a roughness term r to be able to investigate the sensitivity of our model to the melt term and write

$$\frac{\partial K}{\partial t} = \frac{r g \rho_w b K (\nabla h)^2}{L_f \rho_i} - 2 K A \left[\frac{N}{n}\right]^n \tag{A11}$$

and considering unconfined case as well, it is

$$\frac{\partial K}{\partial t} = \frac{r g \rho_w \min(b, h - z_b) K (\nabla h)^2}{L_f \rho_i} - 2 K A \left[\frac{N}{n}\right]^n. \tag{A12}$$

Our reasoning behind scaling K and not b are unintended side effects of changes in b on storage and the behaviour when the aquifer becomes unconfined. A thicker aquifer in areas which represent channels would imply larger storage and also less transmissivity when the area eventually becomes unconfined (because the unconfined case triggers at a higher head already, limiting transmissivity). However, we do not expect the storage to increase, because channels usually do not store a lot of water and pressure changes travel faster than in the inefficient system. Also, the effective system should still have higher transmissivity when the water pressure drops (as long as it does not empty completely).

Appendix B: Discretization

We discretize the transient flow equation (Eq. (3)) on an equidistant rectangular grid using an explicit forward in time central in space (FTCS) finite-difference approximation. For sake of completeness, we give the equations for a non-equidistant grid here.

For the spatial discretization, we use a second-order central difference scheme (e.g., Ferziger and Perić, 2002) leading to the spatial discretization operator for the head $\mathcal{L}_h$:

$$\begin{aligned}\mathcal{L}_h =& T_{i+\frac{1}{2},j} \frac{h_{i+1,j} - h_{i,j}}{(\Delta_f x)_i (\Delta_c x)_i} - T_{i-\frac{1}{2},j} \frac{h_{i,j} - h_{i-1,j}}{(\Delta_b x)_i (\Delta_c x)_i} \\ &+ T_{i,j+\frac{1}{2}} \frac{h_{i,j+1} - h_{i,j}}{(\Delta_f y)_j (\Delta_c y)_j} - T_{i,j-\frac{1}{2}} \frac{h_{i,j} - h_{i,j-1}}{(\Delta_b 1)_j (\Delta_c y)_j} + Q\end{aligned} \tag{B1}$$

where half-grid values of T denote harmonic rather than arithmetic averages computed using Eq. (4), where

$$(\Delta_c x)_k = (x_{k+1} - x_{k-1})/2, \tag{B2}$$

$$(\Delta_f x)_k = x_{k+1} - x_k, \quad \text{and} \tag{B3}$$

$$(\Delta_b x)_k = x_k - x_{k-1} \tag{B4}$$

denote central, forward, and backward differences, respectively. Re-writing this more compactly in compass notation

$$\mathcal{L}_h = d_\mathrm{S} h_\mathrm{S} + d_\mathrm{W} h_\mathrm{W} + d_\mathrm{P} h_\mathrm{P} + d_\mathrm{E} h_\mathrm{E} + d_\mathrm{N} h_\mathrm{N} + Q \tag{B5}$$

with

$$d_\mathrm{W} = \frac{T_{i-\frac{1}{2},j}}{(\Delta x)_i^2},\ d_\mathrm{E} = \frac{T_{i+\frac{1}{2},j}}{(\Delta x)_i^2},\ d_\mathrm{S} = \frac{T_{i,j-\frac{1}{2}}}{(\Delta x)_j^2},\ d_\mathrm{N} = \frac{T_{i,j+\frac{1}{2}}}{(\Delta x)_j^2},$$

$$\text{and} \qquad d_\mathrm{P} = -(d_\mathrm{W} + d_\mathrm{E} + d_\mathrm{S} + d_\mathrm{N}). \tag{B6}$$

We use the explicit Euler method for the time discretization, where the next time step $m+1$ is computed from the previous time step m ($\Delta t = t_{m+1} - t_m$) (using a somewhat sloppy notation)

$$\begin{aligned} h^{m+1} = h^m + \frac{\Delta t}{S_e} \big(& d_\mathrm{S}^m h_\mathrm{S}^m + d_\mathrm{W}^m h_\mathrm{W}^m \\ & + d_\mathrm{P}^m h_\mathrm{P}^m + d_\mathrm{E}^m h_\mathrm{E}^m + d_\mathrm{N}^m h_\mathrm{N}^m - Q^m \big). \end{aligned} \tag{B7}$$

Conductivity is updated in each time step by Eq. (9):

$$K^{m+1} = K^m + \Delta t \left(v_\mathrm{melt}^m - v_\mathrm{creep}^m \right), \tag{B8}$$

where we use a combined forward- backward-difference scheme for the discretization of $(\nabla h)^2$ in Eq. (10):

$$\begin{aligned} (\nabla h)^2 \approx & \frac{1}{2} \left[\left(\frac{h_{i,j} - h_{i-1,j}}{(\Delta_b x)_i} \right)^2 + \left(\frac{h_{i+1,j} - h_{i,j}}{(\Delta_f x)_i} \right)^2 \right. \\ & \left. + \left(\frac{h_{i,j} - h_{i,j-1}}{(\Delta_b y)_j} \right)^2 + \left(\frac{h_{i,j+1} - h_{i,j}}{(\Delta_f y)_j} \right)^2 \right]. \end{aligned} \tag{B9}$$

Compared to central differences, this stencil is more robust at nodes with large heads caused by moulins.

The time step is chosen sufficiently small that the discretization error is dominated by the spatial discretization ~~.~~ (the Courant–Friedrichs–Lewy condition is always satisfied) Additionally, we check that the time step is small enough for the unconfined component of the scheme to become active by restarting the time step with a decreased Δt if at any point $h < z_b$.

All variables are co-located on the same grid, but the conductivity K is evaluated at the midpoints between two grid cells using the harmonic mean due to its better representation of conductivity jumps (e.g. at no-flow boundaries).

A ~~big~~ disadvantage of this discrete formulation is that it is not mass-conservative (see, e.g. Celia et al. (1990)). The solution to this is to use a mixed formulation for Darcy flow in which also the Darcy velocity is solved for. ~~We discuss the consequences of this limitation and leave~~ However, in our application, the resulting error is very small, and we plan to implement the mixed formulation approach ~~for~~ in future work.

Competing interests. The authors declare that they have no conflict of interest.

Acknowledgements. This work is part of the GreenRISE project, a project funded by Leibniz-Gemeinschaft: WGL Pakt für Forschung SAW-2014-PIK-1. We kindly acknowledge the efforts of Basile de Fleurian und Mauro Werder who were designing and supporting the SHMIP project. We highly benefited from their well developed test geometries and fruitful discussions not only at splinter meetings.

We acknowledge A. Aschwanden for providing basal melt rates, temperatures and velocities simulated by PISM. Development of PISM is supported by NASA grants NNX13AM16G, NNX16AQ40G, NNH16ZDA001N and by NSF grants PLR-1644277 and PLR-1603799.

References

Aschwanden, A., Fahnestock, M. A., and Truffer, M.: Complex Greenland outlet glacier flow captured, Nature Communications, 7, https://doi.org/10.1038/ncomms10524, 2016.

Bartholomew, I., Nienow, P., Mair, D., Hubbard, A., King, M. A., and Sole, A.: Seasonal evolution of subglacial drainage and acceleration in a Greenland outlet glacier, Nature Geoscience, 3, 408–411, 2010.

Bondzio, J. H., Morlighem, M., Seroussi, H., Kleiner, T., Rückamp, M., Mouginot, J., Moon, T., Larour, E. Y., and Humbert, A.: The mechanisms behind Jakobshavn Isbræ's acceleration and mass loss: A 3-D thermomechanical model study, Geophysical Research Letters, 44, 6252–6260, https://doi.org/10.1002/2017GL073309, 2017GL073309, 2017.

Bueler, E. and van Pelt, W.: Mass-conserving subglacial hydrology in the Parallel Ice Sheet Model version 0.6, Geoscientific Model Development, 8, 1613–1635, https://doi.org/10.5194/gmd-8-1613-2015, http://www.geosci-model-dev.net/8/1613/2015/, 2015.

Celia, M. A., Bouloutas, E. T., and Zarba, R. L.: A general mass-conservative numerical solution for the unsaturated flow equation, Water Resources Research, 26, 1483–1496, https://doi.org/10.1029/WR026i007p01483, http://dx.doi.org/10.1029/WR026i007p01483, 1990.

Cuffey, K. M. and Paterson, W. S. B.: The physics of Glaciers, Elsevier, Oxford, 4th edn., 2010.

De Fleurian, B., Gagliardini, O., Zwinger, T., Durand, G., Le Meur, E., Mair, D., and Raback, P.: A double continuum hydrological model for glacier applications, Cryosphere, 8, 137–153, https://doi.org/10.5194/tc-8-137-2014, 2014.

de Fleurian, B., Morlighem, M., Seroussi, H., Rignot, E., van den Broeke, M. R., Kuipers Munneke, P., Mouginot, J., Smeets, P. C. J. P., and Tedstone, A. J.: A modeling study of the effect of runoff variability on the effective pressure beneath Russell Glacier, West Greenland, Journal of Geophysical Research: Earth Surface, 121, 1834–1848, https://doi.org/10.1002/2016JF003842, http://dx.doi.org/10.1002/2016JF003842, 2016JF003842, 2016.

Ehlig, C. and Halepaska, J. C.: A numerical study of confined-unconfined aquifers including effects of delayed yield and leakage, Water Resources Research, 12, 1175–1183, https://doi.org/10.1029/WR012i006p01175, http://dx.doi.org/10.1029/WR012i006p01175, 1976.

Fahnestock, M., Abdalati, W., Joughin, I., Brozena, J., and Gogineni, P.: High geothermal heat flow, basal melt, and the origin of rapid ice flow in central Greenland, Science, 294, 2338–2342, https://doi.org/10.1126/science.1065370, 2001.

Ferziger, J. H. and Perić, M.: Computational Methods for Fluid Dynamics, Springer, 3rd edn., 2002.

Flowers, G. E.: Modelling water flow under glaciers and ice sheets, Proceedings of the Royal Society A-mathematical Physical and Engineering Sciences, 471, 20140 907, https://doi.org/10.1098/rspa.2014.0907, 2015.

Fowler, A. C.: Sliding with cavity formation, Journal of Glaciology, 33, 255–267, https://doi.org/10.1017/S0022143000008820, 1987.

Gimbert, F., Tsai, V. C., Amundson, J. M., Bartholomaus, T. C., and Walter, J. I.: Subseasonal changes observed in subglacial channel pressure, size, and sediment transport, Geophysical Research Letters, 43, 3786–3794, 2016.

Goelzer, H., Nowicki, S., Edwards, T., Beckley, M., Abe-Ouchi, A., Aschwanden, A., Calov, R., Gagliardini, O., Gillet-Chaulet, F., Golledge, N. R., Gregory, J., Greve, R., Humbert, A., Huybrechts, P., Kennedy, J. H., Larour, E., Lipscomb, W. H., Le clec′h, S., Lee, V., Morlighem, M., Pattyn, F., Payne, A. J., Rodehacke, C., Rückamp, M., Saito, F., Schlegel, N., Seroussi, H., Shepherd, A., Sun, S., van de Wal, R., and Ziemen, F. A.: Design and results of the ice sheet model initialisation experiments initMIP-Greenland: an ISMIP6 intercomparison, The Cryosphere Discussions, 2017, 1–42, https://doi.org/10.5194/tc-2017-129, https://www.the-cryosphere-discuss.net/tc-2017-129/, 2017.

Hewitt, I. J.: Seasonal changes in ice sheet motion due to melt water lubrication, Earth and Planetary Science Letters, 371, 16–25, https://doi.org/10.1016/j.epsl.2013.04.022, 2013.

Hewitt, I. J., Schoof, C., and Werder, M. A.: Flotation and free surface flow in a model for subglacial drainage. Part 2. Channel flow, Journal of Fluid Mechanics, 702, 157–187, https://doi.org/10.1017/jfm.2012.166, 2012.

Hill, E. A., Carr, J. R., and Stokes, C. R.: A Review of Recent Changes in Major Marine-Terminating Outlet Glaciers in Northern Greenland, Frontiers in Earth Science, 4, 111, https://doi.org/10.3389/feart.2016.00111, https://www.frontiersin.org/article/10.3389/feart.2016.00111, 2017.

Hoffman, M. and Price, S.: Feedbacks between coupled subglacial hydrology and glacier dynamics, Journal of Geophysical Research-earth Surface, 119, 414–436, https://doi.org/10.1002/2013JF002943, 2014.

Hubbard, B., Sharp, M., Willis, I., NIELSEN, M. t., and Smart, C.: Borehole water-level variations and the structure of the subglacial hydrological system of Haut Glacier d'Arolla, Valais, Switzerland, Journal of Glaciology, 41, 572–583, 1995.

Huybrechts, P.: A 3-D model for the Antarctic ice sheet: a sensitivity study on the glacial-interglacial contrast, Climate Dynamics, 5, 79–92, 1990.

Joughin, I., Fahnestock, M., MacAyeal, D., Bamber, J. L., and Gogineni, P.: Observation and analysis of ice flow in the largest Greenland ice stream, Journal of Geophysical Research: Atmospheres, 106, 34 021–34 034, 2001.

Joughin, I., Smith, B. E., Howat, I. M., Scambos, T., and Moon, T.: Greenland flow variability from ice-sheet-wide velocity mapping, Journal of Glaciology, 56, 415–430, 2010.

Kolditz, O., Shao, H., Wang, W., and Bauer, S., eds.: Thermo-Hydro-Mechanical-Chemical Processes in Fractured Porous Media: Modelling and Benchmarking, Springer, 2015.

Larour, E., Seroussi, H., Morlighem, M., and Rignot, E.: Continental scale, high order, high spatial resolution, ice sheet modeling using the Ice Sheet System Model (ISSM), Journal of Geophysical Research: Earth Surface, 117, https://doi.org/10.1029/2011JF002140, 2012.

Lliboutry, L.: General theory of subglacial cavitation and sliding of temperate glaciers, Journal of Glaciology, 7, 21–58, 1968.

MacAyeal, D. R.: Large-scale ice flow over a viscous basal sediment: Theory and application to ice stream B, Antarctica, Journal of Geophysical Research: Solid Earth, 94, 4071–4087, 1989.

Morland, L.: Unconfined ice-shelf flow, Dynamics of the West Antarctic Ice Sheet, 4, 99–116, 1987.

Morlighem, M., Rignot, E., Mouginot, J., Seroussi, H., and Larour, E.: Deeply incised submarine glacial valleys beneath the Greenland ice sheet, Nature Geoscience, 7, 418–422, 2014.

Morlighem, M., Bondzio, J., Seroussi, H., Rignot, E., Larour, E., Humbert, A., and Rebuffi, S.: Modeling of Store Gletscher's calving dynamics, West Greenland, in response to ocean thermal forcing, Geophysical Research Letters, 43, 2659–2666, https://doi.org/10.1002/2016gl067695, 2016.

Nye, J. F.: Water flow in glaciers: Jökulhlaups, tunnels and veins, Journal of Glaciology, 17, 181–207, 1976.

Rignot, E. and Mouginot, J.: Ice flow in Greenland for the international polar year 2008–2009, Geophysical Research Letters, 39, 2012.

Rothlisberger, H.: Water pressure in subglacial channels, in: Union Géodésique et Géophysique Internationale. Association Internationale d'Hydrologie Scientifique. Commission de Neiges et Glaces. Symposium on the hydrology of Glaciers, Cambridge, 7, p. 97, 1969.

Röthlisberger, H.: Water Pressure in Intra- and Subglacial Channels, Journal of Glaciology, 11, 177–203, https://doi.org/10.1017/S0022143000022188, 1972.

Schoof, C.: Ice-sheet acceleration driven by melt supply variability, Nature, 468, 803–806, http://dx.doi.org/10.1038/nature09618, 2010.

Schoof, C., Hewitt, I. J., and Werder, M. A.: Flotation and free surface flow in a model for subglacial drainage. Part 1. Distributed drainage, Journal of Fluid Mechanics, 702, 126–156, 2012.

Shreve, R.: Movement of water in glaciers, Journal of Glaciology, 11, 205–214, 1972.

Vallelonga, P., Christianson, K., Alley, R. B., Anandakrishnan, S., Christian, J. E. M., Dahl-Jensen, D., Gkinis, V., Holme, C., Jacobel, R. W., Karlsson, N. B., Keisling, B. A., Kipfstuhl, S., Kjær, H. A., Kristensen, M. E. L., Muto, A., Peters, L. E., Popp, T., Riverman, K. L., Svensson, A. M., Tibuleac, C., Vinther, B. M., Weng, Y., and Winstrup, M.: Initial results from geophysical surveys and shallow coring of the Northeast Greenland Ice Stream (NEGIS), The Cryosphere, 8, 1275–1287, https://doi.org/10.5194/tc-8-1275-2014, https://www.the-cryosphere.net/8/1275/2014/, 2014.

van den Broeke, M., Box, J., Fettweis, X., Hanna, E., Noël, B., Tedesco, M., van As, D., van de Berg, W. J., and van Kampenhout, L.: Greenland Ice Sheet Surface Mass Loss: Recent Developments in Observation and Modeling, Current Climate Change Reports, pp. 1–12, 2017.

Van Siclen, C. D.: Equivalent channel network model for permeability and electrical conductivity of fracture networks, Journal of Geophysical Research: Solid Earth, 107, ECV 1–1–ECV 1–10, https://doi.org/10.1029/2000JB000057, http://dx.doi.org/10.1029/2000JB000057, 2002.

Weertman, J.: On the sliding of glaciers, J. Glaciol, 3, 33–38, 1957.

Werder, M. A., Hewitt, I. J., Schoof, C. G., and Flowers, G. E.: Modeling channelized and distributed subglacial drainage in two dimensions, Journal of Geophysical Research-earth Surface, 118, 2140–2158, https://doi.org/10.1002/jgrf.20146, 2013.

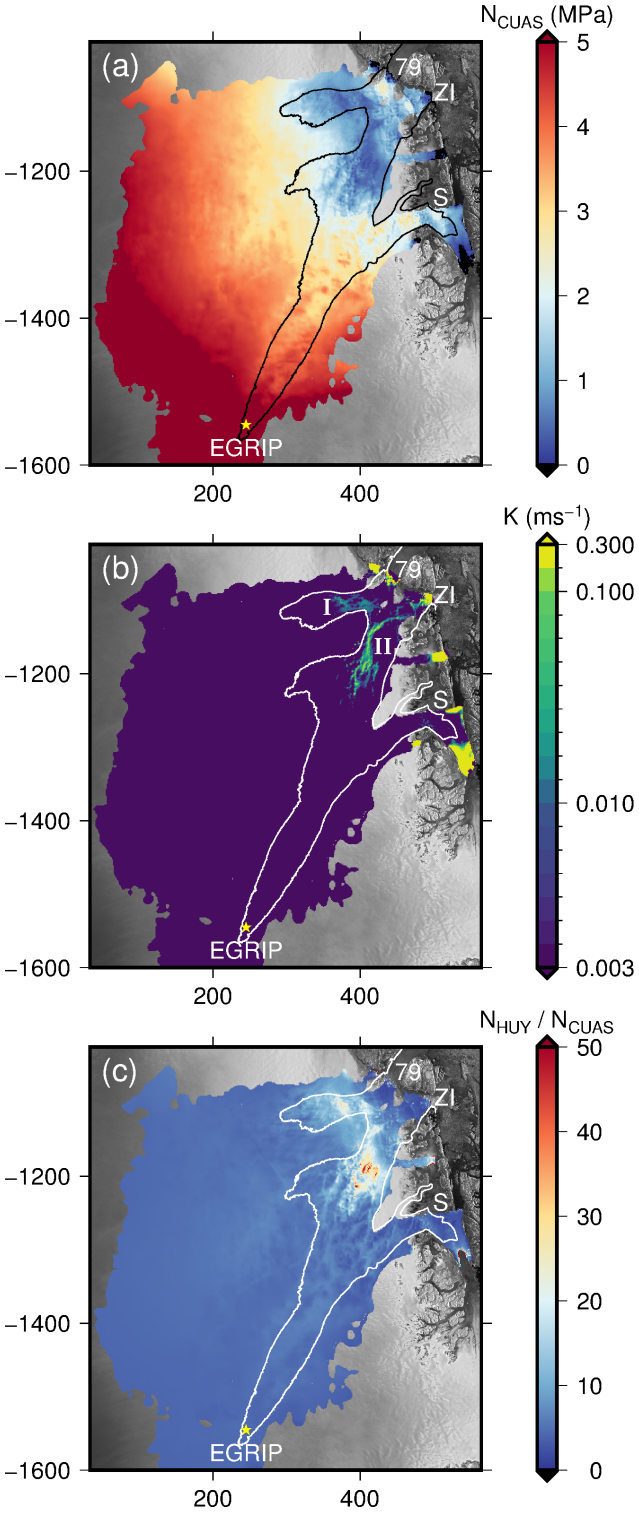

Figure 9. Results for NEGIS region with forcing due to basal melt (PISM) ~~,~~ representing winter conditions. White lines indicate the $50\,\mathrm{m\,a^{-1}}$ velocity contour. Panel (a) shows effective pressure N_{CUAS}, (b) conductivity K (logarithmic scale), and (c) shows the quotient of the ice overburden pressure above flotation and the effective pressure computed by CUAS.

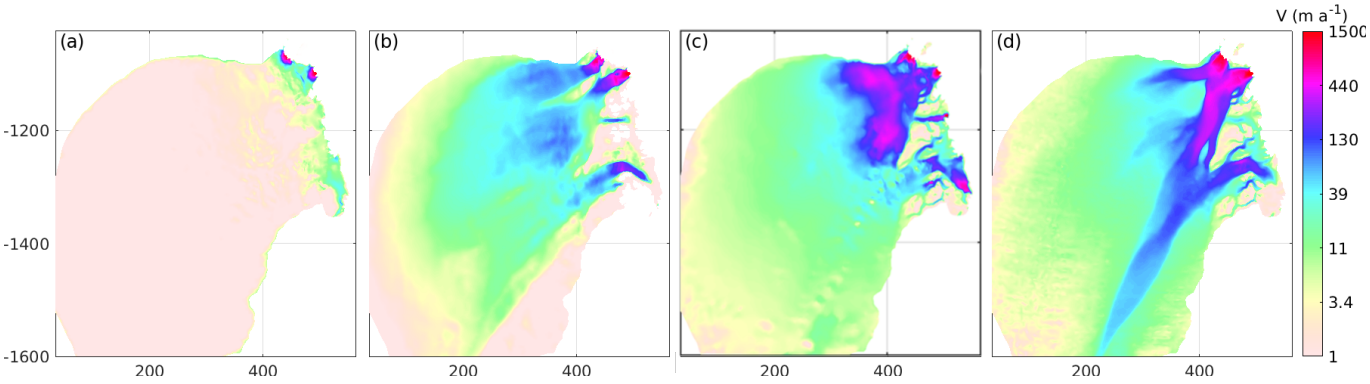

Figure 10. Horizontal surface velocity: ISSM with reduced ice overburden pressure N_{HUY} (a), PISM result from Aschwanden et al. (2016), interpolated to unstructured ISSM grid (b), ISSM with effective pressure from our hydrology model N_{CUAS} (c), and observed velocities (Rignot and Mouginot, 2012) (d).